

# Screening of Clinically Approved and Investigation Drugs as Potential Inhibitors of SARS-CoV-2 Main Protease and Spike Receptor-Binding Domain Bound with ACE2 COVID19 Target Proteins: A Virtual Drug Repurposing Study

Serdar Durdagi<sup>1,\*</sup>, Busecan Aksoydan<sup>1,2</sup>, Berna Dogan<sup>1</sup>, Kader Sahin<sup>1</sup>,  
Aida Shahraki<sup>1,3</sup>, Necla Birgul-Iyison<sup>3</sup>

<sup>1</sup>Computational Biology and Molecular Simulations Laboratory, Department of Biophysics, School of Medicine, Bahcesehir University, Istanbul, Turkey

<sup>2</sup>Neuroscience Program, Graduate School of Health Sciences, Bahçesehir University, Istanbul, Turkey

<sup>3</sup>Department of Molecular Biology and Genetics, Bogazici University, Istanbul, Turkey

---

## Abstract

There is an urgent need for new drugs against COVID-19. Since designing a new drug and testing its pharmacokinetics and pharmacodynamics properties may take years, here we used a physics-driven high throughput virtual screening drug re-purposing approach to identify new compounds against COVID-19. As the molecules considered in repurposing studies passed through several stages and have well-defined profiles, they would not require prolonged pre-clinical studies and hence, they would be excellent candidates in the cases of disease emergencies or outbreaks. While the Spike Protein is the key for the virus to enter the cell through the interaction with ACE2, enzymes such as main protease are crucial for the life cycle of the virus. These proteins are the most attractive targets for the development of new drugs against COVID-19 due to their pivotal roles in the fusion, replication and transcription of the virus. We used 7922 FDA approved small molecule drugs as well as compounds in clinical investigation from NIH Chemical Genomics Center (NCGC) Pharmaceutical Collection (NPC) database in our drug repurposing study. Both apo and holo forms of SARS-CoV-2 Main Proteases as well as Spike protein/ACE2 targets were used in virtual screening. Target proteins were retrieved from protein data bank (PDB IDs, 6M03, 6LU7 and 6M0J). Standard Precision (SP) protocol of Glide docking module of Maestro was used in docking. Compounds were then ranked based on their docking scores that represents binding energies. Top-100 compounds from each docking simulations were considered initially in short (10-ns) molecular dynamics (MD) simulations and their average binding energies were calculated by Molecular Mechanics Generalized Born Surface Area (MM/GBSA) method using collected 1000 trajectories throughout the MD simulations. Promising hit compounds selected based on average MM/GBSA scores were then used in long (100-ns and 500-ns) MD simulations. These numerical calculations showed that the following 8 compounds can be considered as SARS-CoV-2 Main Protease inhibitors: Pimelautide, Rotigaptide, Telinavir, Ritonavir, Pinokalant, Terlakiren, Cefotiam and Cefpiramide. In addition, following 5 compounds were identified as SARS-CoV-2 Spike receptor-binding domain bound with ACE2 inhibitors: Denopamine, Bometolol, Naminterol, Rotigaptide, and Benzquercin. These compounds can be clinically tested and if the simulation results validated, they may be considered to be used as treatment for COVID-19.

---

## \*Corresponding Author:

Prof. Dr. Serdar Durdagi

Computational Biology and Molecular Simulations Laboratory

Department of Biophysics, School of Medicine

Bahcesehir University, Istanbul, 34734, Turkey

[www.durdagilab.com](http://www.durdagilab.com)

[serdar.durdagi@med.bau.edu.tr](mailto:serdar.durdagi@med.bau.edu.tr)

## Introduction

Coronaviruses (CoVs) are the family of viruses containing single-stranded RNA (positive-sense) which is encapsulated by a membrane envelope. They are classified in the Nidovirales order, Coronaviridae family, which is comprised of two sub-families and about 40 known species. These species are divided and characterized into four genera (alpha, beta, gamma and delta), and only the alpha and beta- strains are identified to be pathogenic to human and other mammals<sup>1, 2</sup>. Before 2019, six coronaviruses were known to cause respiratory and enteric diseases in humans, especially the two of them belonging to betaviruse cause severe illness: SARS (Severe Acute Respiratory Syndrome)-CoV and MERS (Middle East Respiratory Syndrome)-CoV. A novel coronavirus is discovered in Wuhan, China in late 2019, and officially named as SARS-CoV-2 (formerly 2019-nCoV) due to its genomic similarity to SARS-CoV<sup>1-4</sup>. The disease caused by this virus is officially named as Coronavirus Disease 2019 (COVID-19) by World Health Organization (WHO). Like SARS- and MERS-CoVs, SARS-CoV-2 mostly affects the lower respiratory tract to cause pneumonia, and may also affect the gastrointestinal system, kidney, heart and central nervous system, with the common symptoms including fever, cough and diarrhea<sup>5</sup>. On 11<sup>th</sup> of March 2020, WHO declared the COVID-19 as pandemic. The first emergence of the virus was witnessed at the penultimate days of 2019 as pneumonia concentrated in Wuhan, China. The outbreak in China was then spread very quickly to the other countries and as of 23<sup>rd</sup> April 2020, more than 2.6 million individuals have been infected by SARS-CoV-2 virus and it is expected that the number will increase in the following months. Thus, drugs and vaccines are highly in demand to control the outbreak.

The genomic sequence of SARS-CoV-2 is available (GenBank ID: MN908947.3) and the initial analyses indicate that the sequence similarity of around 80% and sequence identity of more than 90% with the different essential enzymes found in SARS-CoV. Furthermore, the catalytic sites of the four key enzymes that could be the antiviral targets are vastly conserved between two coronaviruses<sup>6</sup>. SARS-CoV-2 is also reported to have the same cell-entry receptor for infection, ACE2 (Angiotensin-Converting Enzyme 2), as SARS-CoV<sup>7, 8</sup>. The genome of SARS-CoV-2 encodes for different proteins and important ones are 3-chymotrypsin-like protease, 3CLpro *aka* Main Protease, papain-like protease, helicase, and RNA-dependent RNA polymerase which construct the non-structural proteins and Spike glycoproteins which belong to structural proteins<sup>2,9</sup>. While the Spike protein is the key for the virus to enter the cell through the interaction with ACE2, enzymes such as Main Protease are crucial for the life cycle of the virus. These proteins are the most attractive targets for the development of new drugs against SARS-CoV-2 due to their pivotal role in the virus entry into the host cell and replication and transcription of the virus. One of the advantages of targeting these proteins is that although the mutagenesis rate is high in viruses, not many happens in these proteins since any mutation here can be lethal for the virus.

There are more than 100 3D protein structures for SARS-CoV-2, mostly for the Main Protease structure in apo- and holo- states, resolved via X-ray diffraction or cryo-electron microscopy, deposited and available in Protein Data Bank (RCSB PDB). *In silico* studies related to Main Protease are increasing in terms of protein-inhibitor interactions and drug screening<sup>10,11</sup>. For a broad review of additional background, patents, developments and perspectives in COVID-19 and other diseases related to coronavirus, the reader is referred to see<sup>7</sup>.

The phenomenon known as drug repositioning or repurposing has gained attention as the development of new drug starting from the beginning becoming more costly in respect to both time and resources required.<sup>12-15</sup> Established favorable toxicological, pharmacokinetic and

pharmacodynamic properties of approved/clinical drug molecules make them suitable to be used for new indications.<sup>16-19</sup> As the molecules considered in repurposing studies passed through several stages and have well-defined profiles, they would not require prolonged pre-clinical studies and hence, they would be excellent candidates in the cases of disease emergencies or outbreaks.<sup>20-21</sup> Drug repurposing studies have already been conducted for various kind of diseases (review articles for different diseases<sup>16, 21-24</sup>). Thanks to repositioning studies, different compounds have been found new usages than their original purposes<sup>21, 25</sup> even though they have been failed in their original purpose and/or withdrawn from the market.<sup>26</sup> Computational approaches such as virtual screening would decrease the times required for the identification of new targets for the existing drug molecules with the advantage of also being cost-efficient as demonstrated in review articles.<sup>18, 25, 27</sup>

In our group, virtual screening of different ligand databases including FDA approved drugs have been performed vastly in recent years by an in-house script and it is shown that the obtained results by this screening algorithm which is a hybrid algorithm of ligand- and target-driven based screening techniques gave successful results.<sup>28-32</sup> Thus, in the current study, this hybrid algorithm is applied for the identification of approved compounds against SARS-CoV-2 essential target proteins (i.e., Main Protease and Spike receptor-binding domain bound with ACE2).

## Results and Discussion

Main protease has been studied by different groups to find inhibitors capable of halting the activity of this enzyme and consequently the reproduction of the virus. After the SARS outbreak in 2003 many researches were conducted to target the Main Protease of the SARS-CoV. Chen *et al.*<sup>33</sup> utilized screening approaches using a 3D model of SARS-CoV 3CLpro to screen the MDL-CMC database that contains 8.000 compounds. Cinanserin was among the high-ranked final compounds for which *in vitro* studies were performed. The proteolytic activity of the enzyme was shown to be inhibited by 70 to 90% at 50 to 100  $\mu$ M of Cinanserin<sup>34</sup>.

In a study performed by Liu *et al.*<sup>35</sup> homology modeling was used to construct a model of main protease since SARS 3CLPro was not publicly available at the time of the work. Then high throughput virtual screening was performed using different chemical libraries including The National Cancer Institute Diversity Set (230.000 compounds total), ACD-3D (Available Chemical Database, Release: ACD 3D 2002.2, 280.000 compounds in total), and MDDR-3D (MDL Drug Database Report, Release: MDDR 3D 2002.2, 120.000 compounds in total). The final hits (40 compounds) were further tested *in vitro* to check the inhibition activity, and 3 of them were found to inhibit the protease activity up to 40%. C3930 or calmidazolium which is the calmodulin antagonist was found as the best hit with the highest inhibition activity<sup>35</sup>.

After the recent outbreak of SARS-CoV-2, many research groups have started to use screening methods to search for the inhibitors of Main Protease and Spike protein domain/ACE2 complex. In a recent paper, Li *et al.*<sup>36</sup> have screened 8.000 molecules including the approved or experimental compounds and small molecules derived from DrugBank. The protease protein with the PDB ID 5N5O was used as target. Compounds showing better docking score than -7.7 kcal/mol were selected as hits and experimentally unapproved ones, as well as those with strong side effects were removed from the list. The list was even shortened considering the marketability of the molecules. Prulifloxacin, Bictegravir, Nelfinavir and Tegobuvi are finally selected molecules<sup>37</sup>. In a research conducted by Chen *et al.*<sup>38</sup> apo-enzyme structure of SARS-CoV (PDB ID: 2DUC) was used to build a model for the main protease of SARS-CoV-2 and

MTiOpenScreen web service<sup>9</sup> was used to screen for purchasable drugs (Drugs-lib). The library has 7173 compounds. Autodock Vina<sup>39</sup> was used to screen the active site at chains A and B and finally 10 and 11 drugs were selected for these chains respectively based on the energy cut-off.<sup>37</sup> Another recent study conducted by Jin *et al.*<sup>40</sup> targeted the Main Protease as well. This group found some promising compounds by combining structure-based drug design approaches with screening methods. *In vitro* cell-based assays showed the high inhibitory effect of the finally chosen compounds on the target enzyme and antiviral activities. Virtual screening studies were performed by Jin *et al.*<sup>40</sup> using a model constructed based on the crystal structure of SARS-CoV-2 Main Protease in complex with N3 inhibitor (PDB ID: 6LU7). An in-house library containing potential binding compounds was used. Cinanserin was found as the best binding affinity to the substrate-binding pocket of the enzyme, and *in vitro* studies showed an IC<sub>50</sub> of 124.93  $\mu$ M for Cinanserin<sup>40</sup>. Cinanserin, a serotonin antagonist was previously found to inhibit SARS-CoV<sup>34</sup>. Fluorescence Resonance Energy Transfer (FRET)-based high-throughput screening resulted in the finding of some FDA-approved drugs (Disulfiram and Carmofur) and other compounds which are in preclinical/clinical trial (Ebselen, TDZD-8, Shikonin, Tideglusib, and PX-12).<sup>40</sup> In this study, the compound Ebselen was found the most active compound with IC<sub>50</sub> value of 0.48  $\mu$ M.<sup>40</sup>

In the present study, we used 7922 compounds from NIH Chemical Genomics Center (NCGC) Pharmaceutical Collection (NPC) database (<https://tripod.nih.gov/npc/>) and in order to eliminate the non-specific binders, some criteria including molecular weight, between 100 to 1000 g/mol; number of rotatable bonds, <100; number of atoms, between 10 and 100; number of aliphatic and aromatic rings, <10; number of hydrogen-bond acceptor and donors, <10 were set and as a result the total number of compounds was decreased to 6654. These 6654 compounds were then docked to the binding cavities of apo (PDB, 6M03) and holo (PDB, 6LU7) forms of SARS-CoV-2 main protease enzyme. (Figure 1). For the Spike protein/ACE-2 target 6M0J PDB-coded structure was used. In docking, standard precision (SP) protocol of Glide docking module of Schrodinger software was used. Tables S1 and S2 show the top-100 docking scored compounds based on the docking scores at the COVID-19 in holo and apo forms, respectively. Table S3 shows the corresponding docking scores table for Spike protein domain/ACE-2 complex. Although recent studies have suggested that docking is a successful approach for selecting hits, since in the docking approach flexibility of both protein residues and docked ligand are not fully considered, hence the ranking and ordering of the compounds only by their corresponding docking scores may not potentially lead to the identification of correct compounds. Moreover, although molecular docking studies may give an initial insight into protein-ligand interactions, it is always crucial to understand the maintenance of these interactions by performing dynamical studies such as molecular dynamics (MD) simulations. Therefore, we selected top-100 compounds from each docking simulations and initially performed short (10-ns) MD simulations for these complexes (in total 3- $\mu$ s MD simulations via Desmond). An in-house script was used for the preparation of simulation boxes as well as for the analysis of MD simulations. Desmond was used in MD simulations. Tables S4 and S5 represent average MM/GBSA scores using collected 1000 trajectory frames (strided by 10 throughout each simulations) of selected 100 top-docking scored compounds from both holo- and apo- based simulations, respectively. Table S6 shows average MM/GBSA scores of selected top-100 docking scored compounds at Spike Protein/ACE-2 interface. We also performed MD simulations for the co-crystallized ligand-bound structure (inhibitor N3 at PDB ID: 6LU7) using the same MD protocol for screening compounds. Figure S1 shows protein-ligand interaction diagram of inhibitor N3 at the Main Protease. The figure includes a timeline representation of the interactions and contacts (H-bonds, hydrophobic, ionic, water bridges) representing which residues interact with the ligand in each trajectory frame. Interactions that

occur more than 15.0% of the simulation time in the selected trajectory (0.00 through 100.00 ns), are shown. The stacked bar charts are also normalized over the course of the trajectory (i.e., a value of 0.5 suggests that 50% of the simulation time the specific interaction is maintained). Results showed that the following residues are crucial for ligand binding: Thr26, His41, Met49, Asn142, His164, Glu166, Gln189, Thr190 and Gln192. Several water bridges and hydrogen bonding interactions dominate the interaction constructed from Glu166. The interactions between these residues and the screened compounds were also checked. Average MM/GBSA scores of co-crystallized ligand N3 from long MD simulations was found as  $-89.34 \pm 7.68$  kcal/mol. Thus, we forwarded compounds that have better average MM/GBSA scores than a cutoff value ( $-70.0$  kcal/mol) from short MD simulations to long MD simulations. We selected top-21 compounds based on average MM/GBSA scores from short (10-ns) MD simulations performed on holo form main protease target and conducted 100-ns long MD simulations for each. (Table S7) Other selected compounds from short MD simulations such as Arzoxifene and Truxicuriem could not maintain their initial crucial interactions during the simulations. Based on average MM/GBSA scores from 100-ns simulations, we also forwarded 13 compounds to 500-ns MD simulations. (Table S8)

Interestingly, while 21 compounds identified using the target retrieved from holo-state short simulations fit the cutoff value, only 5 compounds were found from database screened at apo-state. Long (100-ns) MD simulations were also performed for compounds screened in apo form Main Protease enzyme and only two compounds were found as promising ligands. (Table S9)

While Table 1 shows identified compounds targeting Main Protease enzyme, Table 2 represents determined compounds at the Spike protein domain/ACE2 interface. As can be seen from Table 1, for main protease enzyme average MM/GBSA scores show that following 11 compounds: Pinokalant, Bms181176-14, Terlakiren, Bisnafide, Ritonavir, Cefotiam, Telinavir, Rotigaptide, Cefpiramide, Lopinavir and Pimelautide have significant average MM/GBSA scores, and throughout the MD simulations the interaction between these compounds and the crucial residues of the target were maintained. (Figures S2-S12). Figures S13-S16 represent ligand interactions diagrams for the identified compounds at Spike Protein/ACE2 interface. Following 5 compounds were identified as hit ligands at the Spike Protein/ACE2 doamin: Denopamine, Bometolol, Rotigaptide, Benzquercin and Naminterol.

Interestingly, Rotigaptide was identified as promising compound both in Main Protease and Spike protein/ACE2 targets. Identified compound Rotigaptide is a drug under clinical investigation for the treatment of cardiac arrhythmias – specifically atrial fibrillation. Crucial residue interactions were formed by Thr26, His41, Glu166, Gln189 and Gln192. (Figure S9) Three of the identified compounds at the Main Protease target (Ritonavir, Lopinavir and Telinavir) have been used in clinical studies for HIV infection, while Cefotiam and Cefpiramide are antibiotics. Another identified compound at the Main Protease was Pimelautide which is an immunostimulant and its built-in adjuvants are associated with an HIV-1-derived peptide. Terlakiren and Pinokalant are other identified compounds at the Main Protease which have anti-hypertensive and broad-spectrum cation channel blocker profile, respectively. Two of the identified molecules at the Main Protease (Bms181176-14 and Bisnafide) were used in clinical studies as anti-cancer compounds. Thus, their usage in COVID19 may not be suggested.

We identified 5 compounds at the Spike protein/ACE2 region. Three of them (Denopamine, Bometolol, Naminterol) are compounds targeting beta-adrenergic receptors. As it is mentioned, Rotigaptide is another compound which strongly binds both Spike Protein/ACE2 and Main

Protease targets. In addition, a flavonoid compound Benzquercin was found as strong binder at the Spike Protein/ACE2 region.

## Conclusions

In this virtual drug repurposing study, we used 7922 FDA approved drugs and compounds in clinical investigation from NPC database. Both apo and holo forms of SARS-CoV-2 Main Protease as well as Spike Protein/ACE2 were used for virtual screening. Initially, docking was performed for these compounds at target binding sites. The compounds were then sorted according to their docking scores which represent binding energies. The first 100 compounds from each docking simulations were initially subjected to short (10 ns) MD simulations (in total 300 ligand-bound complexes), and average binding energies during MD simulations were calculated using the MM/GBSA method. Then, the selected promising hit compounds based on average MM/GBSA scores were used in long (100-ns and 500-ns) MD simulations. In total around 15  $\mu$ s MD simulations were performed in this study. Both docking and MD simulations binding free energy calculations showed that holo form of the target protein is more appropriate choice for virtual drug screening studies. These numerical calculations have shown that the following 8 compounds can be considered as SARS-CoV-2 Main Protease inhibitors: Pimelautide, Rotigaptide, Telinavir, Ritonavir, Pinokalant, Terlakiren, Cefotiam and Cefpiramide. In addition, following 5 compounds were identified as potential SARS-CoV-2 ACE-2/Spike protein domain inhibitors: Denopamine, Bometolol, Naminterol, Rotigaptide and Benzquercin. These compounds can be clinically tested and if the simulation results validated, they may be considered to be used as treatment for COVID-19.

## Methods

7922 compounds were downloaded from NPC database (<https://tripod.nih.gov/npc/>). In order to eliminate the non-specific binders, some criteria including molecular weight, between 100 to 1000 g/mol; number of rotatable bonds, <100; number of atoms, between 10 and 100; number of aliphatic and aromatic rings, <10; number of hydrogen-bond acceptor and donors, <10 were set and as a result the total number of compounds was decreased to 6654. These ligands were prepared using LigPrep module of Maestro at neutral pH (LigPrep, Schrodinger v.2017). In molecular docking, we used following protein structures: apo-Main Protease, (PDB, 6M03); holo-Main Protease, (PDB, 6LU7); and Spike Protein/ACE-2, (PDB, 6M0J). These proteins were prepared using Protein Preparation module of Maestro. PROPKA was used for determination of protonation states of amino acid residues. Restrained minimization was performed with OPLS3 force field for the protein using 0.3 Å heavy atom convergence. Docking was performed with Glide/SP using default settings. Protein-ligand complexes were placed in the orthorhombic boxes with explicit TIP3P water models that have 10 Å thickness from the edges of target proteins. All systems were neutralized and 0.15 M NaCl salt solution added to the systems. The long-range electrostatic interactions were calculated by the particle mesh Ewald method. A cut-off radius of 9 Å was used for both van der Waals and Coulombic interactions. Simulations were performed at body temperature (310 K) and 1.01325 bar. Nose-Hoover thermostat<sup>41</sup> and Martyna-Tobias-Klein barostat<sup>42</sup> was used at the simulations. The time step was 2 fs. The OPLS3 force field was used in simulations. Throughout the MD simulations, 1000 trajectory frames (for 10-ns and 100-ns simulations) and 2000 trajectory frames (for 500-ns simulations) were recorded and Molecular Mechanics Generalized Born Surface Area (MM/GBSA) binding free energies of compounds were calculated. VSGB 2.0 solvation model at Prime module of Maestro was utilized during MM/GBSA calculations.

## References

1. Chen, Y.; Liu, Q.; Guo, D., Emerging coronaviruses: genome structure, replication, and pathogenesis. *Journal of medical virology* 2020.
2. Paules, C. I.; Marston, H. D.; Fauci, A. S., Coronavirus infections—more than just the common cold. *Jama* 2020, 323, 707-708.
3. Hui, D. S.; I Azhar, E.; Madani, T. A.; Ntoumi, F.; Kock, R.; Dar, O.; Ippolito, G.; Mchugh, T. D.; Memish, Z. A.; Drosten, C., The continuing 2019-nCoV epidemic threat of novel coronaviruses to global health—The latest 2019 novel coronavirus outbreak in Wuhan, China. *International Journal of Infectious Diseases* 2020, 91, 264-266.
4. Song, Z.; Xu, Y.; Bao, L.; Zhang, L.; Yu, P.; Qu, Y.; Zhu, H.; Zhao, W.; Han, Y.; Qin, C., From SARS to MERS, thrusting coronaviruses into the spotlight. *Viruses* 2019, 11, 59.
5. Liu, C.; Zhou, Q.; Li, Y.; Garner, L. V.; Watkins, S. P.; Carter, L. J.; Smoot, J.; Gregg, A. C.; Daniels, A. D.; Jervey, S., In; ACS Publications: 2020.
6. Liu, W.; Morse, J. S.; Lalonde, T.; Xu, S., Learning from the past: possible urgent prevention and treatment options for severe acute respiratory infections caused by 2019-nCoV. *Chembiochem* 2020.
7. Cao, Y.; Li, L.; Feng, Z.; Wan, S.; Huang, P.; Sun, X.; Wen, F.; Huang, X.; Ning, G.; Wang, W., Comparative genetic analysis of the novel coronavirus (2019-nCoV/SARS-CoV-2) receptor ACE2 in different populations. *Cell Discovery* 2020, 6, 1-4.
8. Chen, J., Pathogenicity and transmissibility of 2019-nCoV—a quick overview and comparison with other emerging viruses. *Microbes and infection* 2020.
9. Li, G.; De Clercq, E., In; Nature Publishing Group: 2020.
10. Khaerunnisa, S.; Kurniawan, H.; Awaluddin, R.; Suhartati, S.; Soetjipto, S., Potential Inhibitor of COVID-19 Main Protease (Mpro) From Several Medicinal Plant Compounds by Molecular Docking Study. 2020.
11. Ryo, H.; Koji, O.; Yuji, M.; Kaori, F.; Yuto, K.; Yoshio, O.; Shigenori, T., Fragment Molecular Orbital Based Interaction Analyses on COVID-19 Main Protease - Inhibitor N3 Complex (PDB ID:6LU7). 2020.
12. Adams, C. P.; Brantner, V. V., Estimating the cost of new drug development: is it really \$802 million? *Health affairs* 2006, 25, 420-428.
13. DiMasi, J. A.; Florez, M. I.; Stergiopoulos, S.; Peña, Y.; Smith, Z.; Wilkinson, M.; Getz, K. A., Development times and approval success rates for drugs to treat infectious diseases. *Clinical Pharmacology & Therapeutics* 2020, 107, 324-332.
14. DiMasi, J. A.; Grabowski, H. G.; Hansen, R. W., Innovation in the pharmaceutical industry: new estimates of R&D costs. *Journal of health economics* 2016, 47, 20-33.
15. Scannell, J. W.; Blanckley, A.; Boldon, H.; Warrington, B., Diagnosing the decline in pharmaceutical R&D efficiency. *Nature reviews Drug discovery* 2012, 11, 191.
16. Abdelaleem, M.; Ezzat, H.; Osama, M.; Megahed, A.; Alaa, W.; Gaber, A.; Shafei, A.; Refaat, A., Prospects for repurposing CNS drugs for cancer treatment. *Oncology reviews* 2019, 13.
17. Corsello, S. M.; Bittker, J. A.; Liu, Z.; Gould, J.; McCarren, P.; Hirschman, J. E.; Johnston, S. E.; Vrcic, A.; Wong, B.; Khan, M., The Drug Repurposing Hub: a next-generation drug library and information resource. *Nature medicine* 2017, 23, 405-408.
18. Ma, D.-L.; Chan, D. S.-H.; Leung, C.-H., Drug repositioning by structure-based virtual screening. *Chemical Society Reviews* 2013, 42, 2130-2141.
19. Oprea, T. I.; Bauman, J. E.; Bologna, C. G.; Buranda, T.; Chigaev, A.; Edwards, B. S.; Jarvik, J. W.; Gresham, H. D.; Haynes, M. K.; Hjelle, B., Drug repurposing from an academic perspective. *Drug Discovery Today: Therapeutic Strategies* 2011, 8, 61-69.

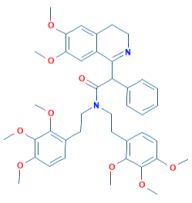
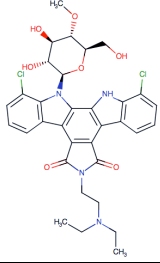
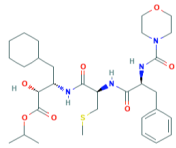
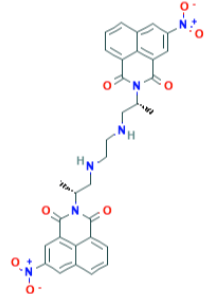
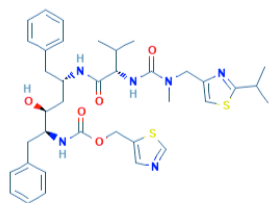
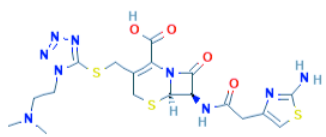
20. Chong, C. R.; Sullivan, D. J., New uses for old drugs. *Nature* 2007, 448, 645-646.
21. Zheng, W.; Sun, W.; Simeonov, A., Drug repurposing screens and synergistic drug-combinations for infectious diseases. *British journal of pharmacology* 2018, 175, 181-191.
22. Andrews, K. T.; Fisher, G.; Skinner-Adams, T. S., Drug repurposing and human parasitic protozoan diseases. *International Journal for Parasitology: Drugs and Drug Resistance* 2014, 4, 95-111.
23. Pizzorno, A.; Padey, B.; Terrier, O.; Rosa-Calatrava, M., Drug repurposing approaches for the treatment of influenza viral infection: Reviving old drugs to fight against a long-lived enemy. *Frontiers in immunology* 2019, 10, 531.
24. Yadav, V.; Talwar, P., Repositioning of fluoroquinolones from antibiotic to anti-cancer agents: An underestimated truth. *Biomedicine & Pharmacotherapy* 2019, 111, 934-946.
25. Nowak-Sliwinska, P.; Scapozza, L.; Altaba, A. R., Drug repurposing in oncology: Compounds, pathways, phenotypes and computational approaches for colorectal cancer. *Biochimica et Biophysica Acta (BBA)-Reviews on Cancer* 2019.
26. Ashburn, T. T.; Thor, K. B., Drug repositioning: identifying and developing new uses for existing drugs. *Nature reviews Drug discovery* 2004, 3, 673-683.
27. Dudley, J. T.; Deshpande, T.; Butte, A. J., Exploiting drug-disease relationships for computational drug repositioning. *Briefings in bioinformatics* 2011, 12, 303-311.
28. Tutumlu G, Dogan B, Avsar T, Orhan MD, Calis S, Durdagi S. Integrating Ligand and Target-Driven Based Virtual Screening Approaches with in vitro human Cell Line Models to Identify Novel Hit Compounds Against BCL-2. *Frontiers in Chemistry* 2020, DOI: 10.3389/fchem.2020.00167
29. Ikram S, Ahmad J, Durdagi S. Screening of FDA approved drugs for finding potential inhibitor for Granzyme B as a potent drug-repurposing target. *Journal of Molecular Graphics and Modeling* 2020. DOI: 10.1016/j.jmgm.2019.107462.
30. Kanan T, Kanan D, Erol I, Yazdi S, Stein M, Durdagi S. Targeting the NF- $\kappa$ B/I $\kappa$ B $\alpha$  Complex via Fragment-Based E-Pharmacophore Virtual Screening and Binary QSAR Models. *Journal of Molecular Graphics and Modelling* 2019, 86, 264-277.
31. Is YS, Durdagi S, Aksoydan B, Yurtsever M. Proposing Novel MAO-B Hit Inhibitors Using Multidimensional Molecular Modeling Approaches and Application of Binary QSAR Models for Prediction of their Therapeutic Activity and Toxic Effects. *ACS Chemical Neuroscience* 2018, 9(7), 1768-1782.
32. Durdagi S, Aksoydan B, Erol I, Kantarcioglu I, Ergun Y, Bulut G, Acar M, Avsar T, Liapakis G, Karageorgos V, Salmas RE, Sergi B, Alkhatib S, Turan G, Yigit BF, Cantasir K, Kurt B, Kilic T. Integration of Multi-scale Molecular Modeling Approaches with Experiments for the in silico Guided Design and Discovery of Novel hERG-Neutral Antihypertensive Oxazolone and Imidazolone Derivatives and Analysis of Their Potential Restrictive Effects on Cell Proliferation. *European Journal of Medicinal Chemistry* 2018;145:273-290
33. Shoichet, B. K.; McGovern, S. L.; Wei, B.; Irwin, J. J., Lead discovery using molecular docking. *Current opinion in chemical biology* 2002, 6, 439-446.
34. Chen, L.; Gui, C.; Luo, X.; Yang, Q.; Günther, S.; Scandella, E.; Drosten, C.; Bai, D.; He, X.; Ludewig, B., Cinanserin is an inhibitor of the 3C-like proteinase of severe acute respiratory syndrome coronavirus and strongly reduces virus replication in vitro. *Journal of virology* 2005, 79, 7095-7103.
35. Liu, Z.; Huang, C.; Fan, K.; Wei, P.; Chen, H.; Liu, S.; Pei, J.; Shi, L.; Li, B.; Yang, K., Virtual screening of novel noncovalent inhibitors for SARS-CoV 3C-like proteinase. *Journal of chemical information and modeling* 2005, 45, 10-17.

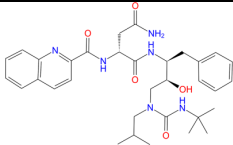
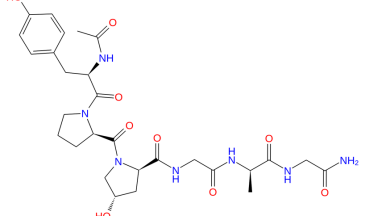
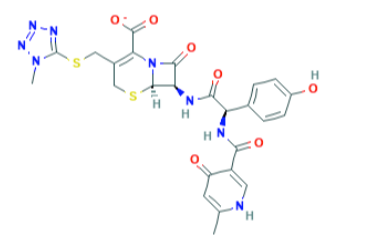
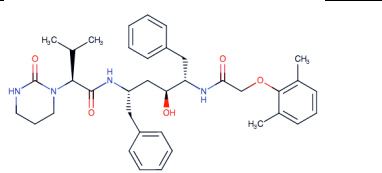
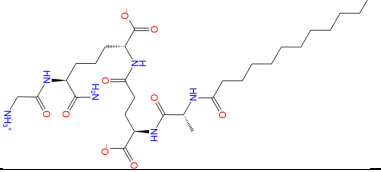


36. Wishart, D. S.; Feunang, Y. D.; Guo, A. C.; Lo, E. J.; Marcu, A.; Grant, J. R.; Sajed, T.; Johnson, D.; Li, C.; Sayeeda, Z., DrugBank 5.0: a major update to the DrugBank database for 2018. *Nucleic acids research* 2018, 46, D1074-D1082.
37. Li, Y.; Zhang, J.; Wang, N.; Li, H.; Shi, Y.; Guo, G.; Liu, K.; Zeng, H.; Zou, Q., Therapeutic Drugs Targeting 2019-nCoV Main Protease by High-Throughput Screening. *bioRxiv* 2020.
38. Labbé, C. M.; Rey, J.; Lagorce, D.; Vavruša, M.; Becot, J.; Sperandio, O.; Villoutreix, B. O.; Tufféry, P.; Miteva, M. A., MTiOpenScreen: a web server for structure-based virtual screening. *Nucleic acids research* 2015, 43, W448-W454.
39. Trott, O.; Olson, A. J., AutoDock Vina: improving the speed and accuracy of docking with a new scoring function, efficient optimization, and multithreading. *Journal of computational chemistry* 2010, 31, 455-461.
40. Jin, Z.; Du, X.; Xu, Y.; Deng, Y.; Liu, M.; Zhao, Y.; Zhang, B.; Li, X.; Zhang, L.; Duan, Y., Structure-based drug design, virtual screening and high-throughput screening rapidly identify antiviral leads targeting COVID-19. *bioRxiv* 2020.
41. Evans DJ; Holian BL. The Nose–Hoover thermostat. *J. Chem. Phys.* 83, 4069 (1985); DOI: 10.1063/1.449071
42. Martyna GJ, Tobias DJ, Klein ML. Constant pressure molecular dynamics algorithms. *J. Chem. Phys.* 1994, 101 (5),4177.

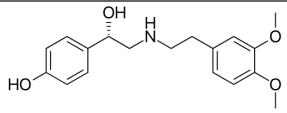
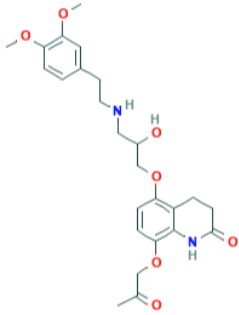
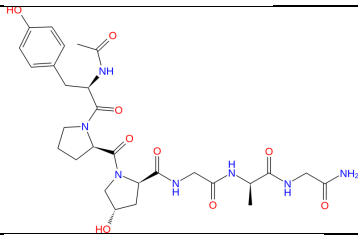
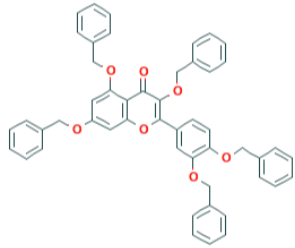
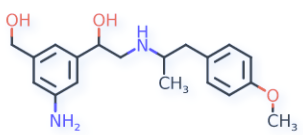
## Tables

**Table 1.** Selected hit compounds based on average MM/GBSA scores at Main Protease target. Long (100-ns and 500-ns) MD simulations are performed for these identified hits and average MM/GBSA scores were calculated using 1000-trajectory frames (2000-trajectory frames for 500-ns) throughout the simulations. Table also shows the corresponding mechanism of actions of the identified compounds.

Compounds	2D Structures	MM/GBSA (kcal/mol)	Mechanism of Action
Pinokalant		-87.57	Broad-spectrum cation channel blocker
Bms181176-14 (Becatecarin)		-87.56	Becatecarin is a small molecule, anticancer compound for the treatment of hepatobiliary duct tumors
Terlakiren		-86.89	Antihypertensive, Renin inhibitor
Bisnafide		-84.54	Bisnafide is a bis-naphthalimide compound with anticancer activity.
Ritonavir		-83.22	Ritonavir is an antiretroviral protease inhibitor
Cefotiam		-82.24	Cefotiam is a parenteral second-generation cephalosporin antibiotic

<b>Telinavir</b>		-80.87	Telinavir is an anti-HIV aspartyl protease inhibitor
<b>Rotigaptide</b>		-78.53	Rotigaptide (ZP-123) is a drug under clinical investigation for the treatment of cardiac arrhythmias – specifically atrial fibrillation.
<b>Cefpiramide</b>		-78.35	Cefpiramide is a third-generation cephalosporin antibiotic.
<b>Lopinavir</b>		-68.92	Lopinavir is an antiretroviral of the protease inhibitor.
<b>Pimelautide</b>		-68.83	Immunostimulant. Pimelautide Built-in Adjuvants Associated with an HIV-1-Derived Peptide

**Table 2.** Selected hit compounds based on average MM/GBSA scores at ACE-2/Spike Protein domain. Long (100-ns) MD simulations are performed for these identified hits and average MM/GBSA scores were calculated using 1000-trajectory frames throughout the simulations. Table also shows the corresponding mechanism of actions of the identified compounds.

Compounds	2D Structures	MM/GBSA (kcal/mol)	Mechanism of Action
Denopamine		-79.63	Denopamine (INN) is a cardiotonic drug which acts as a $\beta_1$ adrenergic receptor agonist.
Bometolol		-79.47	beta-adrenergic blocking agent
Rotigaptide		-75.10	Rotigaptide (ZP-123) is a drug under clinical investigation for the treatment of cardiac arrhythmias – specifically atrial fibrillation.
Benzquercin		-70.81	A flavonoid compound
Naminterol		-69.20	Naminterol is a $\beta_2$ adrenoceptor agonist with bronchodilatory properties.

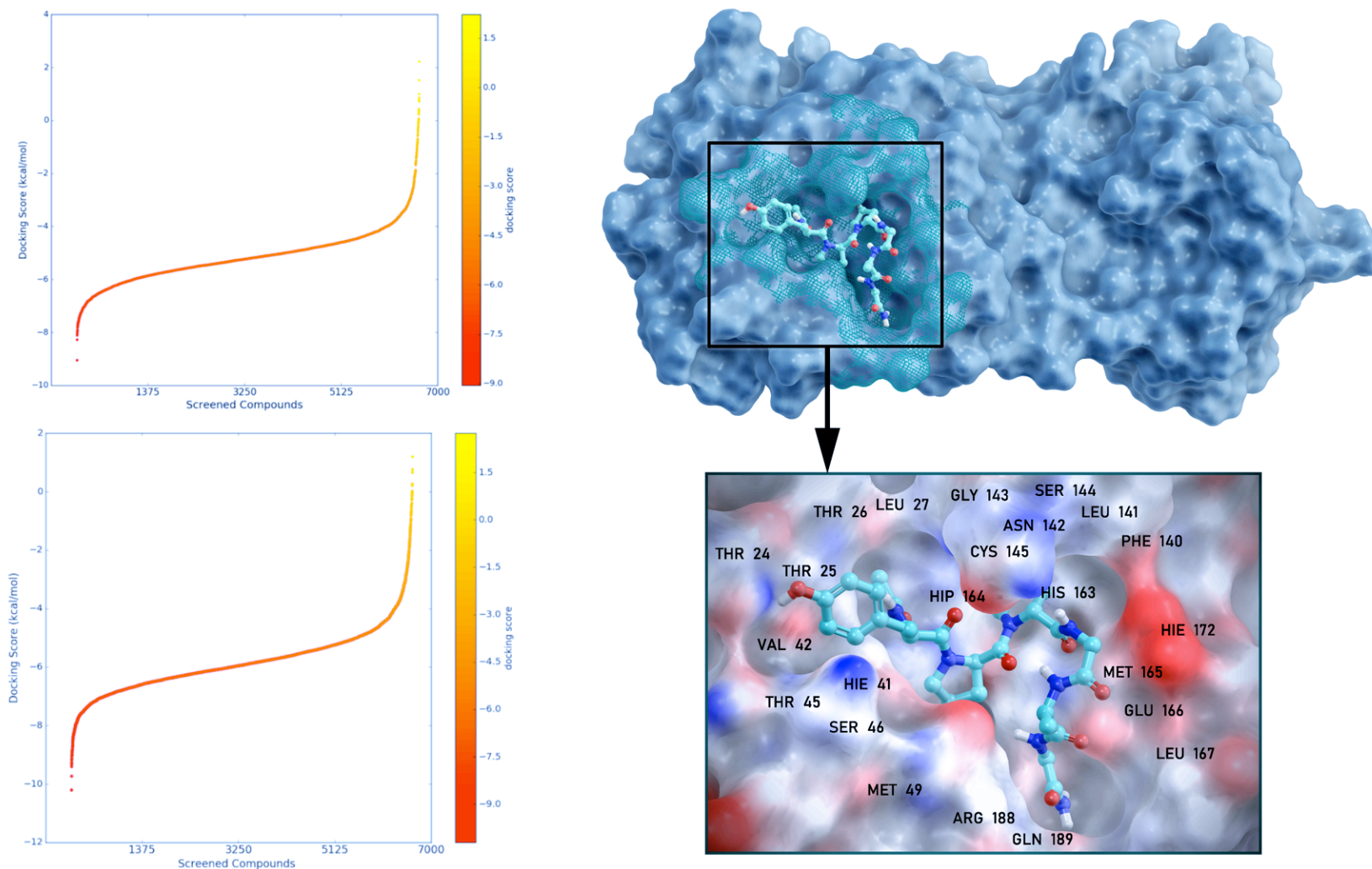


**Figure 1.** Around 7000 FDA approved and drugs in clinical investigation from NPC database were screened at the apo (top-left) and holo (bottom-left) COVID-19 Main Protease target. Hierarchical hybrid screening constructed by our group led to 8 hit compounds. Surface representation of one the identified hit compound Rotigaptide is shown in right.

## Supplementary Materials

# Screening of Clinically Approved and Investigation Drugs as Potential Inhibitors of SARS-CoV-2 Main Protease and Spike Receptor-Binding Domain Bound with ACE2 COVID19 Target Proteins: A Virtual Drug Repurposing Study

Serdar Durdagi<sup>1,\*</sup>, Busecan Aksoydan<sup>1,2</sup>, Berna Dogan<sup>1</sup>, Kader Sahin<sup>1</sup>,

Aida Shahraki<sup>1,3</sup>, Necla Birgul-Iyison<sup>3</sup>

<sup>1</sup>Computational Biology and Molecular Simulations Laboratory, Department of Biophysics, School of Medicine, Bahcesehir University, Istanbul, Turkey

<sup>2</sup>Neuroscience Program, Graduate School of Health Sciences, Bahçeşehir University, Istanbul, Turkey

<sup>3</sup>Department of Molecular Biology and Genetics, Bogazici University, Istanbul, Turkey

### **\*Corresponding Author:**

Prof. Dr. Serdar Durdagi

Computational Biology and Molecular Simulations Laboratory

Department of Biophysics, School of Medicine

Bahcesehir University, Istanbul, 34734, Turkey

[www.durdagilab.com](http://www.durdagilab.com)

[serdar.durdagi@med.bau.edu.tr](mailto:serdar.durdagi@med.bau.edu.tr)

**Table S1.** Top-100 compounds at the binding pocket of SARS-CoV-2 Main Protease crystallized in holo-form (PDB, 6LU7) based on Glide/SP docking scores and their corresponding docking scores.

<b>Compounds</b>	<b>Docking Score (kcal/mol)</b>
Truxipicuriu iodide	-10.209
Ametantrone	-9.736
Arzoxifene	-9.405
Tert-amyloxycarbonyltetraastrin	-9.324
mitoxantrone	-9.270
Ingliforib	-9.178
Frakefamide	-9.134
Pimelautide	-9.041
Truxicuriu	-9.026
Rotigaptide	-9.009
Metkephamid	-8.998
1,3-Bis-(2-ethoxycarbonylchromon-5-yloxy)-2-(lysyloxy)propane	-8.926
Mioflazinum	-8.913
Telinavir	-8.903
Alvimopan	-8.899
Ociltide	-8.896
Azimilide	-8.856
Penimepicycline	-8.839
flupenthixol	-8.817
loglucol	-8.748
Prezatidicupriciacetas	-8.721
Bazedoxifene	-8.701
Losoxantrone	-8.684
Brecanavir	-8.678
Xantifibrate	-8.598
Diathymosulfonum	-8.548
Ledoxantrone	-8.512
Carafiban	-8.476
Efegatran	-8.461
Iohexol	-8.448
Pipendoxifene	-8.447
Sampatrilat	-8.437
Bialamicol	-8.404
Pinoxepin	-8.394
Demecariumbromide	-8.391
Teloxantrone	-8.373

<b>Tetragastrin</b>	-8.352
<b>Bms181176-14</b>	-8.338
<b>Utibapril</b>	-8.301
<b>Zy-15051</b>	-8.292
<b>Epicainide</b>	-8.291
<b>Genestein</b>	-8.289
<b>Aspoxicillin</b>	-8.289
<b>Ftorpropazine</b>	-8.286
<b>14-Benzodioxin-2-methanolalphaalpha'-(iminobis(methylene))bis(2 3-dihydro)-stereoisomer methanesulfonate</b>	-8.283
<b>Bisnafide</b>	-8.282
<b>Flutiazin</b>	-8.274
<b>Etanterol</b>	-8.270
<b>Mefloquine</b>	-8.269
<b>Proflazepam</b>	-8.263
<b>Imidazolidinylureamonosodium</b>	-8.256
<b>ritonavir</b>	-8.226
<b>Montirelin</b>	-8.223
<b>Lu-79553</b>	-8.220
<b>Osutidine</b>	-8.204
<b>R1634</b>	-8.204
<b>Pinokalant</b>	-8.196
<b>Piroxantrone</b>	-8.184
<b>Reproterol</b>	-8.175
<b>Tigecycline</b>	-8.165
<b>Alatrofloxacin</b>	-8.145
<b>Carbuterol</b>	-8.138
<b>Ibutamoren</b>	-8.136
<b>Solabegron</b>	-8.124
<b>Benzilonium</b>	-8.121
<b>Nofecainide</b>	-8.121
<b>Spiclomazinum</b>	-8.094
<b>Lopinavir</b>	-8.083
<b>Topixantrone</b>	-8.081
<b>taltirelin</b>	-8.080
<b>Terlakiren</b>	-8.068
<b>Rolitetracycline</b>	-8.056
<b>Asimadoline</b>	-8.053
<b>Lasinavir</b>	-8.051
<b>Iopamidol</b>	-8.043
<b>Cilengitide</b>	-8.039
<b>Pixantrone</b>	-8.023



<b>Bamifylline</b>	-8.010
<b>2-Chloro-9-(3-dimethylaminopropyl)-9h-thioxanthen-9-ol</b>	-8.003
<b>Remikiren</b>	-8.003
<b>Fludazoniumchloride</b>	-7.997
<b>Pd-196860</b>	-7.994
<b>Butocrolol</b>	-7.993
<b>loversol</b>	-7.963
<b>5-(1-Methyl-4-piperidyl)-5h-dibenzo[ad]cyclohepten-5-olhydrochloride</b>	-7.963
<b>loxilan</b>	-7.952
<b>Glufosfamide</b>	-7.950
<b>Moditeneanthate</b>	-7.947
<b>posaconazole</b>	-7.945
<b>2-[Benzyl(tert-butyl)amino]-1-(a4-dihydroxy-m-tolyl)ethanol</b>	-7.938
<b>Alpiropride</b>	-7.934
<b>Flecainide</b>	-7.933
<b>Ambamustine</b>	-7.932
<b>Ra-233</b>	-7.932
<b>amisulpride</b>	-7.931
<b>Rebimastat</b>	-7.930
<b>Flestolol</b>	-7.927
<b>Capromorelin</b>	-7.921
<b>Difluaninehydrochloride</b>	-7.917
<b>Ecopladib</b>	-7.909

**Table S2.** Top-100 compounds at the binding pocket of SARS-CoV-2 Main Protease crystallized in apo-form (PDB, 6M03) based on Glide/SP docking scores and their corresponding docking scores.

<b>Compounds</b>	<b>Docking Score (kcal/mol)</b>
Ametantrone	-9.211
Teloxantrone	-9.053
mitoxantrone	-8.279
Rotigaptide	-8.113
Pixantrone	-8.065
2-(3,4-Dihydroxyphenyl)-3,5,7-trihydroxy-4h-chromen-4-one	-8.038
5,7,3,4-Tetrahydroxyflavan-3'4'-diol	-7.976
Isoericacid	-7.965
Emiglitate	-7.942
Prospidiumchloride	-7.938
Etanterol	-7.920
loglunide	-7.824
Olmidinehydrochloride (-)-isomer	-7.782
Sibrafiban	-7.763
Fluprostenol	-7.730
Chrysarobin	-7.726
Osutidine	-7.706
Benzyl(tert-butyl)(4-hydroxy-3-hydroxymethyl-4-oxophenethyl) ammonium chloride	-7.687
Cefapirin	-7.685
Difebarbamate	-7.680
Donitriptan	-7.653
Ioxilan	-7.649
Losoxantrone	-7.645
Lasinavir	-7.635
Ociltide	-7.633
Isatoribine	-7.613
Lu-79553	-7.603
Nepafenac	-7.601
Cantabiline	-7.595
Pd-196860	-7.586
Clopthixol	-7.571
Iotriside	-7.570
Netivudine	-7.565
Toldimfos	-7.564
Adosopine	-7.563
Difluaninehydrochloride	-7.536

Emivirine	-7.530
Cifostodine	-7.510
Fenprostalene	-7.488
Dinoprost	-7.487
Reproterol	-7.481
Beta-d-glucopyranoside-4-hydroxyphenyl	-7.464
5-Chloro-1-(4-(4,4-bis(p-fluorophenyl)butyl)-4-piperidyl)-2-benzimidazolinone	-7.459
Orotirelin	-7.451
Prezatidicuprici acetat	-7.451
cladribine	-7.447
Vesnarinone	-7.439
Carboprost	-7.432
arformoterol	-7.431
Tusigen	-7.420
Primoziida	-7.418
Enprostil	-7.416
Nordefrin	-7.396
D-glycero-D-gulo-Heptonicacid	-7.390
Fenoterol	-7.384
Torbafylline	-7.382
Doreptide	-7.381
Tilisolol	-7.361
Lobucavir	-7.361
Ilomastat	-7.349
Eganoprost	-7.348
Eplivanserin	-7.338
(1R2R)-2-amino-1-(4-methylsulfonylphenyl)propane-1,3-diol	-7.332
Sapropterin	-7.331
Odiparcilum	-7.328
Arabinosylthymine	-7.325
Cicarperone	-7.323
Tetragastrin	-7.312
Iohexol	-7.299
Telinavir	-7.297
Nofecainide	-7.291
Prostalene	-7.282
Lasofloxifene	-7.279
Spasfon-lyoc	-7.277
Cefradine	-7.275
Resorcinoldisodium	-7.271
Tiaprost	-7.267

<b>1,4-Benzodioxin-2-methanolalpha alpha'-(iminobis(methylene))bis(2 3-dihydro)-stereoisomer methanesulfonate</b>	-7.258
<b>Fidarestat</b>	-7.255
<b>Temoporfin</b>	-7.254
<b>Glucosulfamide</b>	-7.251
<b>cefotiam</b>	-7.251
<b>Maribavir</b>	-7.248
<b>Sulprostone</b>	-7.243
<b>1,3-Bis-(2-ethoxycarbonylchromon-5-yloxy)-2-(lysoxy)propane</b>	-7.241
<b>Iliparcil</b>	-7.238
<b>Zy-15051</b>	-7.237
<b>Adenosine</b>	-7.228
<b>Ibutamoren</b>	-7.225
<b>Beciparcil</b>	-7.216
<b>Tigecycline</b>	-7.215
<b>Midodrine</b>	-7.204
<b>Cefpiramide</b>	-7.201
<b>Cefetecol</b>	-7.196
<b>Soquinolol</b>	-7.194
<b>Mioflazinum</b>	-7.193
<b>Ceforanide</b>	-7.193
<b>Carafiban</b>	-7.186
<b>Piroxantrone</b>	-7.186
<b>Eptaplatin</b>	-7.171

**Table S3.** Top-100 compounds at the binding pocket of SARS-CoV-2 ACE-2/Spike protein (PDB, 6M0J) based on Glide/SP docking scores and their corresponding docking scores.

<b>Compounds</b>	<b>Docking Score (kcal/mol)</b>
Lasinavir	-7.879
Ametantrone	-7.723
Metoxamina	-7.659
Oxiracetam	-7.535
Bometolol	-7.383
arformoterol	-7.320
Emiglitate	-7.313
Tigecycline	-7.271
mitoxantrone	-7.256
Piroxantrone	-7.198
Teloxantrone	-7.193
Toborinone	-7.185
Prostalene	-7.172
N-methyl-3-4-methylenedioxyphenethylamine hydrochloride	-7.154
3-Pyridinemethanol	-7.140
Azanidazole	-7.103
Ociltide	-7.093
1-3-Benzodioxole-5-ethanamine alpha-methyl-	-7.091
Xamoterol	-7.066
Sulfinalol	-7.062
Ampholytg	-7.059
Fosmenic acid	-7.049
Cefpiramide	-7.044
Tetragastrin	-7.038
Rotigaptide	-6.989
Stiripentol	-6.955
2-Amino-6-chloropurine	-6.928
Tert-amyloxycarbonyltetragastrin	-6.924
formoterol	-6.922
1-3-Bis-(2-ethoxycarbonylchromon-5-yloxy)-2-(lysyloxy)propane	-6.922
Arildone	-6.911
Denopamine	-6.909
Cletoquine	-6.902
Nifurpirinol	-6.888
Norbudrine	-6.886
Protokylol	-6.882

<b>2-Pyridinemethanol</b>	-6.879
<b>Tranilast</b>	-6.876
<b>Istradefylline</b>	-6.875
<b>Nitrofurantoin</b>	-6.871
<b>Toldimfos</b>	-6.851
<b>Cefpimizole</b>	-6.850
<b>Losoxantrone</b>	-6.847
<b>Dopamine</b>	-6.842
<b>Puromycin</b>	-6.839
<b>Penimepicycline</b>	-6.824
<b>Meclocycline</b>	-6.821
<b>valganciclovir</b>	-6.801
<b>Osemozotan</b>	-6.801
<b>Epinephrine acetate</b>	-6.789
<b>Flurocitabine</b>	-6.774
<b>Morforex</b>	-6.768
<b>Uracil</b>	-6.759
<b>Iralukast</b>	-6.753
<b>cianidanol</b>	-6.738
<b>loglucol</b>	-6.727
<b>Acetryptinum</b>	-6.719
<b>Buciclovir</b>	-6.705
<b>Tiaprost</b>	-6.701
<b>2-<sub>3</sub>-4-Dihydroxyphenyl-<sub>3</sub>-<sub>5</sub>-7-trihydroxy-4h-chromen-4-one</b>	-6.693
<b>Naminterol</b>	-6.683
<b>Pixantrone</b>	-6.681
<b>Enloplatin</b>	-6.677
<b>3-4-Dimethoxyphenethylamine</b>	-6.675
<b>Cangrelor</b>	-6.669
<b>Silibinin</b>	-6.660
<b>Xantifibrate</b>	-6.640
<b>B4 vitamini</b>	-6.627
<b>Metostilenol</b>	-6.621
<b>Brecanavir</b>	-6.619
<b>2-4-Diaminohypoxanthine</b>	-6.615
<b>Eptaplatin</b>	-6.605
<b>3-4-Dimethoxy-<math>\alpha</math>-methylphenethylamine</b>	-6.596
<b>1-Ethyl-1-4-dihydro-4-oxo-1-3-dioxolo[4-5-g]cinnoline-3-carbonitrile</b>	-6.589
<b>Zatebradine</b>	-6.581
<b>Methoxyamphetamine</b>	-6.580
<b>Lu-79553</b>	-6.573

<b>1-2-Benzenedicarboxaldehyde</b>	-6.561
<b>Ruboxistaurin</b>	-6.556
<b>Zoxazolaminum</b>	-6.545
<b>Citolone</b>	-6.544
<b>Creatinine</b>	-6.542
<b>Metkephamid</b>	-6.541
<b>Ala-pro</b>	-6.522
<b>3-5-Dihydroxyanisole</b>	-6.514
<b>Bms181176-14</b>	-6.514
<b>5-Oxo-l-proline p-hydroxyphenyl ester</b>	-6.513
<b>Medroxalol</b>	-6.511
<b>Mipbrandofoxaceprol</b>	-6.501
<b>Nifekalant</b>	-6.496
<b>Xylose</b>	-6.491
<b>Benzquercin</b>	-6.489
<b>Piridicillin sodium</b>	-6.489
<b>Eniluracil</b>	-6.482
<b>Spiperone</b>	-6.476
<b>Gluconolactone</b>	-6.470
<b>Noreximide</b>	-6.468
<b>1-(3-(1-3-Benzodioxol-5-yl)-1-oxo-2-propenyl)-piperidine</b>	-6.454
<b>Fludarabine</b>	-6.451
<b>Nifurvidine</b>	-6.446

**Table S4.** Average binding free energies (MM/GBSA scores) of selected top-100 compounds from docking at the SARS-CoV-2 Main protease crystallized in holo form. 1000 trajectory frames were considered throughout the short (10-ns) MD simulations.

<b>Compounds</b>	<b>MM/GBSA (kcal/mol)</b>
Ritonavir	-113,19
Bms181176-14	-90,70
Lopinavir	-87,17
Pimelautide	-83,71
Rotigaptide	-81,21
Bisnafide	-80,40
Fludazoniumchloride	-80,25
Remikiren	-79,52
Truxicarium	-78,58
Ioversol	-78,19
Terlakiren	-77,84
Pinokalant	-77,80
Tert-amylloxycarbonyltetragastrin	-76,71
1,3-Bis-(2-ethoxycarbonylchromon-5-yloxy)-2-(lysyloxy)propane	-76,59
Brecanavir	-74,83
Arzoxifene	-74,35
Ociltide	-74,3
Osutidine	-71,50
Ibutamoren	-71,45
Lasinavir	-71,40
Telinavir	-70,13
Ioxilan	-69,23
Ecopladib	-68,06
Rebimastat	-67,63
Frakefamide	-67,54
posaconazole	-67,52
Truxipicarium iodide	-67,38
Carafiban	-67,26
Tigecycline	-66,58
1-4-Benzodioxin-2-methanolalphaalpha'-(iminobis(methylene))bis(2 3-dihydro)- stereoisomer methanesulfonate	-66,51
Demecariumbromide	-65,63
Zy-15051	-64,78



<b>5-(1-Methyl-4-piperidyl)-5h-dibenzo[ad]cyclohepten-5-olhydrochloride</b>	-64,05
<b>Aspoxicillin</b>	-63,48
<b>Ambamustine</b>	-63,47
<b>Benzilonium</b>	-63,29
<b>Asimadoline</b>	-62,40
<b>Tetragastrin</b>	-62,36
<b>Lu-79553</b>	-61,73
<b>Metkephamid</b>	-61,33
<b>Diathymosulfonum</b>	-60,84
<b>Penimepicycline</b>	-60,76
<b>2-[Benzyl(tert-butyl)amino]-1-(a4-dihydroxy-m-tolyl)ethanol</b>	-60,65
<b>Mioflazinum</b>	-59,03
<b>Epicaïnide</b>	-58,93
<b>Topixantrone</b>	-58,88
<b>Piroxantrone</b>	-56,93
<b>Montirelin</b>	-56,84
<b>Ra-233</b>	-55,90
<b>Difluaninehydrochloride</b>	-55,72
<b>Ingliforib</b>	-55,04
<b>Azimilide</b>	-54,68
<b>Iopamidol</b>	-54,64
<b>2-Chloro-9-(3-dimethylaminopropyl)-9h-thioxanthen-9-ol</b>	-54,58
<b>Butocrolol</b>	-54,53
<b>Efegatran</b>	-54,26
<b>Sampatrilat</b>	-53,46
<b>Pinoxepin</b>	-53,01
<b>Flestolol</b>	-52,78
<b>Ioglucol</b>	-52,63
<b>Utibapril</b>	-52,61
<b>Rolitetracycline</b>	-52,51
<b>Cilengitide</b>	-52,04
<b>Bamifylline</b>	-51,97
<b>Capromorelin</b>	-51,91
<b>Nofecainide</b>	-51,25
<b>Teloxantrone</b>	-50,86
<b>Solabegron</b>	-50,67
<b>Reproterol</b>	-50,63
<b>R1634</b>	-50,54

<b>Bialamicol</b>	-50,34
<b>mitoxantrone</b>	-50,13
<b>Prezaticupriciacetas</b>	-48,56
<b>Glufosfamide</b>	-48,48
<b>Moditenenantate</b>	-48,47
<b>Iohexol</b>	-48,18
<b>Pixantrone</b>	-47,80
<b>Alvimopan</b>	47,57
<b>Ametantrone</b>	-47,57
<b>flupenthixol</b>	-47,37
<b>Alatrofloxacin</b>	-47,30
<b>Pipendoxifene</b>	-46,99
<b>amisulpride</b>	-46,96
<b>Mefloquine</b>	-46,86
<b>Etanterol</b>	-46,85
<b>Imidazolidinylureamonosodium</b>	-46,54
<b>Spiclomazinum</b>	-45,96
<b>Ftorpropazine</b>	-45,70
<b>Pd-196860</b>	-43,79
<b>Alpiropride</b>	-43,04
<b>taltirelin</b>	-42,62
<b>Proflazepam</b>	-42,47
<b>Flecainide</b>	-41,84
<b>Genestein</b>	-37,86
<b>Bazedoxifene</b>	-37,85
<b>Losoxantrone</b>	-36,40
<b>Carbuterol</b>	-36,19
<b>Flutiazin</b>	-35,86
<b>Ledoxantrone</b>	-32,26
<b>Xantifibrate</b>	-32,19

**Table S5.** Average binding free energies (MM/GBSA scores) of selected top-100 compounds from docking at the SARS-CoV-2 Main protease crystallized in apo form. 1000 trajectory frames were considered throughout the short (10-ns) MD simulations.

<b>Compounds</b>	<b>MM/GBSA (kcal/mol)</b>
Cefpiramide	-77,88
Telinavir	-77,11
Lasinavir	-73,58
Temoporfin	-70,17
cefotiam	-69,86
Mioflazinum	-68,86
loglunide	-67,04
Tigecycline	-66,81
Enprostil	-64,98
Osutidine	-64,55
Ociltide	-63,79
1,3-Bis-(2-ethoxycarbonylchromon-5-yloxy)-2-(lysyloxy)propane	-63,37
loxilan	-61,83
Torbafylline	-60,72
Iotriside	-60,14
Emiglitate	-60,12
Ametantrone	-59,64
Iosericacid	-59,38
Fluprostenol	-58,18
Zy-15051	-57,35
arformoterol	-57,32
Eganoprost	-57,18
Ilomastat	-56,92
Difebarbamate	-56,78
5-Chloro-1-(4-(4,4-bis(p-fluorophenyl)butyl)-4-piperidyl)-2-benzimidazolinone	-56,34
Carafiban	-56,17
Lasofoxifene	-56,12
Cefetecol	-55,92
Prostalene	-55,36
mitoxantrone	-55,08
Ibutamoren	-55,03
Fenprostalene	-53,30
Sulprostone	-52,90
Doreptide	-52,53

Tetragastrin	-52,33
Benzyl(tert-butyl)(4-hydroxy-3-hydroxymethyl-4-oxophenethyl) ammonium chloride	-51,21
Clopentixol	-51,08
Primoza	-50,71
Ceforanide	-50,53
2-(3,4-Dihydroxyphenyl)-3,5,7-trihydroxy-4h-chromen-4-one	-50,08
Iliparil	-49,92
Pd-196860	-49,69
Tusigen	-48,99
1,4-Benzodioxin-2-methanolalpha alpha'-(iminobis(methylene))bis(2 3-dihydro)- stereoisomer methanesulfonate	-48,84
Sibrafiban	-48,67
Losoxantrone	-48,67
Carboprost	-48,53
Fenoterol	-48,22
Rotigaptide	-47,64
Netivudine	-47,36
Tilisolol	-47,15
Orotirelin	-47,02
Lu-79553	-46,52
Teloxantrone	-46,51
Nofecainide	-46,19
Maribavir	-46,09
Odiparilum	-45,62
Dinoprost	-45,37
Vesnarinone	-45,08
Adosopine	-45,00
Tiaprost	-44,92
Emivirine	-44,84
Donitriptan	-44,41
Difluaninehydrochloride	-43,33
cladribine	-43,17
Cicarperone	-43,01
Beciparil	-42,48
Etanterol	-42,35
Nepafenac	-40,44
Isatoribine	-38,91
Fidarestat	-38,58
Adenosine	-38,41
(1R2R)-2-amino-1-(4-methylsulfonylphenyl)propane-1 3-diol	-38,11

Reproterol	-36,60
Pixantrone	-36,58
Nordefrin	-36,50
Prezatidicuprici acetat	-36,14
5,7,3,4-Tetrahydroxyflavan-3'4'-diol	-35,96
Arabinosylthymine	-35,58
Soquinolol	-35,43
Lobucavir	-34,75
Chrysarobin	-34,66
Glucosulfamid	-34,49
Sapropterin	-33,93
Midodrine	-33,59
Iohexol	-33,07
Eplivanserin	-32,39
Cefapirin	-32,08
Cifostodine	-31,26
Piroxantrone	-29,99
Prospidiumchlorid	-28,81
Olmidinehydrochlorid (-)-isomer	-27,91
Cefradine	-21,30
Resorcinoldisodium	-18,89
Cantabiline	-17,45
Spasfon-lyoc	-14,36
D-glycero-D-gulo-Heptonicacid	-13,20
Beta-d-glucopyranosid-4-hydroxyphenyl	-11,38
Toldimfos	-11,28
Eptaplatin	-3,54

**Table S6.** Average binding free energies (MM/GBSA scores) of selected top-100 compounds from docking at the SARS-CoV-2 ACE-2/Spike Protein. 1000 trajectory frames were considered throughout the short (10-ns) MD simulations.

<b>Compounds</b>	<b>MM/GBSA (kcal/mol)</b>
<b>Benzquercin</b>	-95,20
<b>Zatebradine</b>	-89,40
<b>Bometolol</b>	-84,75
<b>Denopamine</b>	-79,98
<b>Rotigaptide</b>	-74,61
<b>Naminterol</b>	-73,59
<b>Sulfinalol</b>	-71,54
<b>Istradefylline</b>	-69,51
<b>Prostalene</b>	-69,17
<b>Cletoquine</b>	-66,65
<b>Cefpiramide</b>	-65,00
<b>Ampholytg</b>	-63,23
<b>Lasinavir</b>	-62,81
<b>Toborinone</b>	-62,76
<b>Piroxantrone</b>	-62,61
<b>Piridicillin sodium</b>	-62,19
<b>Xamoterol</b>	-61,86
<b>Arildone</b>	-61,05
<b>Ociltide</b>	-60,81
<b>Tert-amylloxycarbonyltetragastrin</b>	-60,77
<b>Emiglitate</b>	-59,81
<b>formoterol</b>	-59,69
<b>Tranilast</b>	-57,74
<b>Nifekalant</b>	-57,62
<b>Brecanavir</b>	-56,04
<b>1-3-Bis-(2-ethoxycarbonylchromon-5-yloxy)-2-(lysyloxy)propane</b>	-54,991
<b>Tiaprost</b>	-53,55
<b>Metostilenol</b>	-53,38
<b>3-4-Dimethoxyphenethylamine</b>	-53,34
<b>Nifurpirinol</b>	-53,16
<b>Iralukast</b>	-52,93
<b>Nifurvidine</b>	-51,73
<b>Bms181176-14</b>	-51,60

<b>Ruboxistaurin</b>	-50,11
<b>Buciclovir</b>	-49,89
<b>Morforex</b>	-49,81
<b>Spiperone</b>	-49,71
<b>Norbudrine</b>	-49,65
<b>Losoxantrone</b>	-49,26
<b>Metoxamina</b>	-49,20
<b>Xantifibrate</b>	-49,16
<b>5-Oxo-l-proline p-hydroxyphenyl ester</b>	-49,15
<b>1-(3-(1-3-Benzodioxol-5-yl)-1-oxo-2-propenyl)-piperidine</b>	-48,98
<b>arformoterol</b>	-48,93
<b>Stiripentol</b>	-48,90
<b>Azanidazole</b>	-48,68
<b>3-4-Dimethoxy--ø-methylphenethylamine</b>	-48,04
<b>Tigecycline</b>	-47,92
<b>N-methyl-3-4-methylenedioxyphenethylamine hydrochloride</b>	-47,80
<b>Osemozotan</b>	-47,27
<b>Protokylol</b>	-47,21
<b>Oxiracetam</b>	-47,08
<b>Fludarabine</b>	-46,70
<b>Dopamine</b>	-46,42
<b>Tetragastrin</b>	-45,23
<b>loglucol</b>	-45,17
<b>valganciclovir</b>	-45,08
<b>Ametantrone</b>	-43,05
<b>Metkephamid</b>	-42,02
<b>Epinephrine acetate</b>	-41,96
<b>Pixantrone</b>	-41,69
<b>1-3-Benzodioxole-5-ethanamine alpha-methyl-</b>	-41,46
<b>Medroxalol</b>	-41,23
<b>cianidanol</b>	-41,19
<b>Noreximide</b>	-41,14
<b>Teloxantrone</b>	-40,41
<b>Xylose</b>	-40,25
<b>B4 vitamini</b>	-39,90
<b>Ala-pro</b>	-39,58
<b>Lu-79553</b>	-39,37
<b>1-Ethyl-1-4-dihydro-4-oxo-1-3-dioxolo[4-5-g]cinnoline-3-carbonitrile</b>	-39,32

<b>Gluconolactone</b>	-39,04
<b>Silibinin</b>	-38,35
<b>2-_3_4-Dihydroxyphenyl_-3_5_7-trihydroxy-4h-chromen-4-one</b>	-38,23
<b>Eniluracil</b>	-38,13
<b>Cefpimizole</b>	-37,58
<b>2-Pyridinemethanol</b>	-37,39
<b>Penimepicycline</b>	-37,37
<b>Nitrofurantoin</b>	-37,18
<b>Methoxyamphetamine</b>	-36,32
<b>Flurocitabine</b>	-35,81
<b>2-Amino-6-chloropurine</b>	-35,14
<b>Zoxazolaminum</b>	-33,72
<b>Mipbrandofoxaceprol</b>	-33,26
<b>3-5-Dihydroxyanisole</b>	-32,92
<b>Puromycin</b>	-32,71
<b>Enloplatin</b>	-31,38
<b>mitoxantrone</b>	-31,35
<b>1-2-Benzenedicarboxaldehyde</b>	-30,82
<b>Citolone</b>	-30,46
<b>Uracil</b>	-30,37
<b>3-Pyridinemethanol</b>	-30,19
<b>Cangrelor</b>	-29,82
<b>2-4-Diaminohypoxanthine</b>	-29,80
<b>Creatinine</b>	-29,06
<b>Meclocycline</b>	-27,72
<b>Acetryptinum</b>	-21,53
<b>Toldimfos</b>	-12,88
<b>Fosmenic acid</b>	-9,59
<b>Eptaplatin</b>	8,19



**Table S7.** Average binding free energies (MM/GBSA scores) of selected top-21 compounds from short MD simulations at the SARS-CoV-2 Main protease crystallized in holo form. 1000 trajectory frames were considered throughout long (100-ns) MD simulations.

<b>Compounds</b>	<b>MM/GBSA (kcal/mol)</b>
Ritonavir	-79,33
Bms181176-14	-92,22
Terlakiren	-88,92
Rotigaptide	-86,81
Bisnafide	-85,78
Pinokalant	-83,06
Lasinavir	-80,59
Pimelautide	-76,17
1,3-Bis-(2-ethoxycarbonylchromon-5-yloxy)-2-(lysyloxy)propane	-75,59
Lopinavir	-75,43
Telinavir	-74,22
Brecanavir	-74,06
Fludazoniumchloride	-72,14
Ociltide	-67,35
Remikiren	-64,85
Arzoxifene	-62,37
loversol	-62,24
Tert-amylloxycarbonyltetragastrin	-61,44
Truxicarium	-55,42
Ibutamoren	-49,35
Osutidine	-45,06

**Table S8.** Average binding free energies (MM/GBSA scores) of selected top-13 compounds from 100-ns MD simulations at the SARS-CoV-2 Main protease crystallized in holo form. 1000 trajectory frames were considered throughout long (500-ns) MD simulations.

<b>Compounds</b>	<b>MM/GBSA (kcal/mol)</b>
<b>Pinokalant</b>	-87,57
<b>Bms181176-14</b>	-87,56
<b>Terlakiren</b>	-86,89
<b>Bisnafide</b>	-84,54
<b>Ritonavir</b>	-83,22
<b>Telinavir</b>	-80,87
<b>Rotigaptide</b>	-78,53
<b>Lopinavir</b>	-68,92
<b>Pimelautide</b>	-68,83
<b>Brecanavir</b>	-61,18
<b>Fludazoniumchloride</b>	-59,88
<b>Lasinavir</b>	-57,70
<b>1,3-Bis-(2-ethoxycarbonylchromon-5-yloxy)-2-(lysyloxy)propane</b>	-50,07

**Table S9.** Average binding free energies (MM/GBSA scores) of selected top-5 compounds from 10-ns MD simulations at the SARS-CoV-2 Main protease crystallized in apo form. 1000 trajectory frames were considered throughout the long (100-ns) MD simulations.

<b>Compounds</b>	<b>MM/GBSA (kcal/mol)</b>
<b>Cefotiam</b>	-82.24
<b>Cefpiramide</b>	-78.35
<b>Telnavir</b>	-56.50
<b>Temoporfin</b>	-52.43
<b>Lasinavir</b>	-50.85

**Table S10.** Average binding free energies (MM/GBSA scores) of selected top-8 compounds from short (10-ns) MD simulations at the SARS-CoV-2 ACE-2/Spike Protein. 1000 trajectory frames were considered throughout the long (100-ns) MD simulations.

<b>Compounds</b>	<b>MM/GBSA (kcal/mol)</b>
<b>Denopamine</b>	-79.63
<b>Bometolol</b>	-79.47
<b>Rotigaptide</b>	-75.10
<b>Benzquercin</b>	-70.81
<b>Naminterol</b>	-69.20
<b>Istradefylline</b>	-66.64
<b>Zatebradine</b>	-57.99
<b>Sulfinalol</b>	-54.78

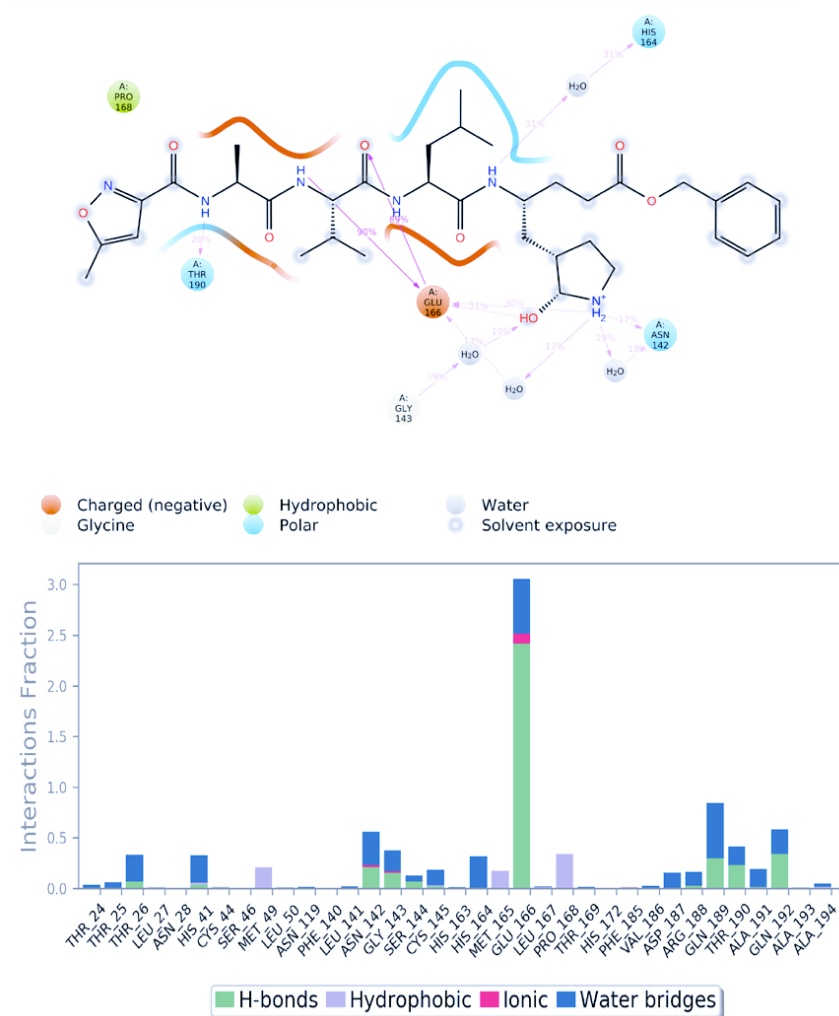
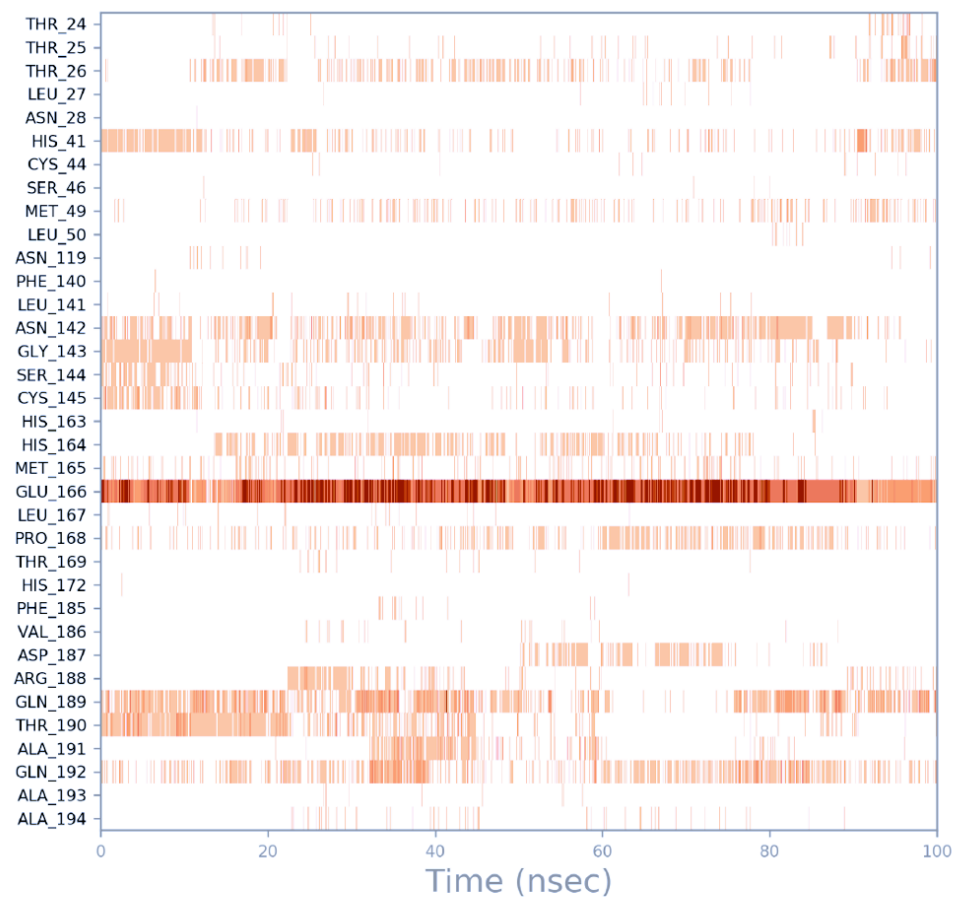


**Figure S1.** Ligand interactions diagram for co-crystallized ligand N3.

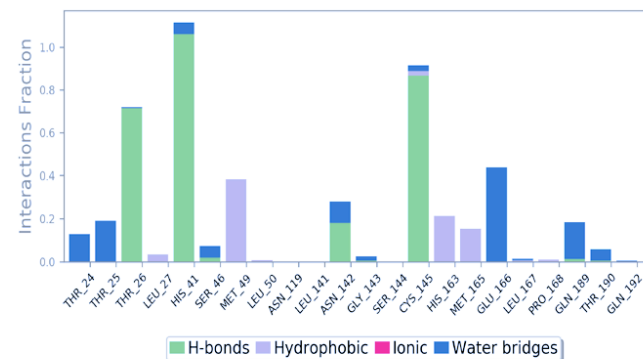
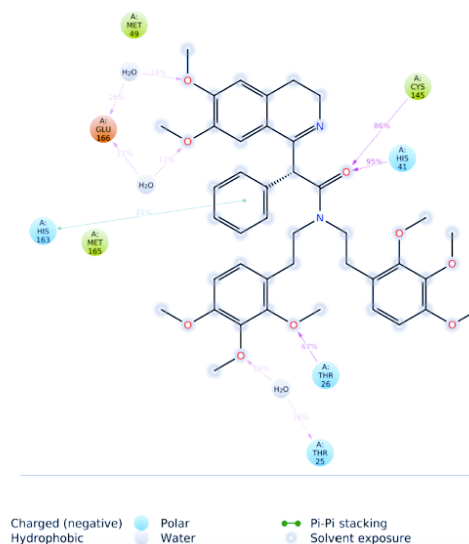
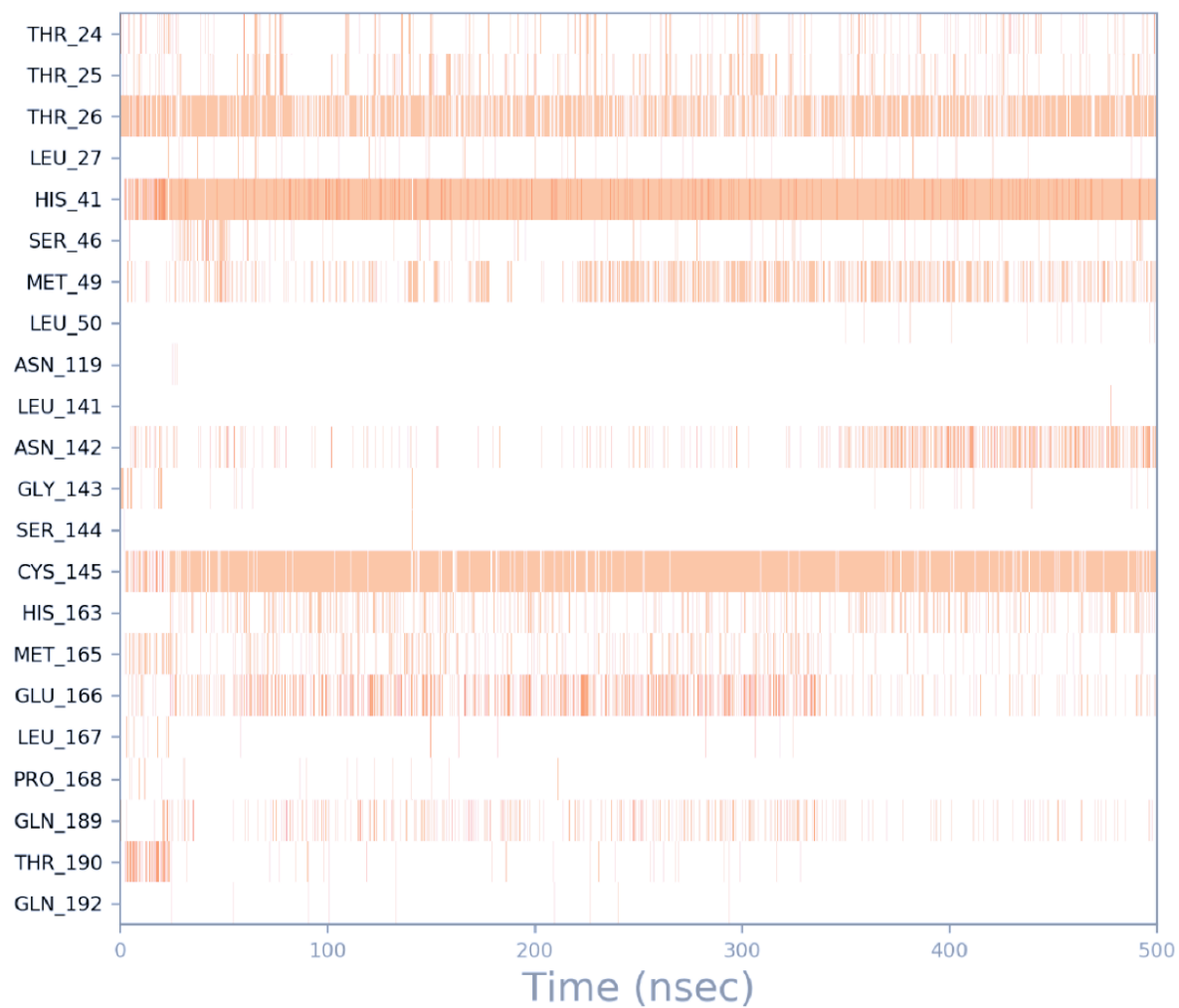


**Figure S2.** Ligand interactions diagram for **Pinokalant**

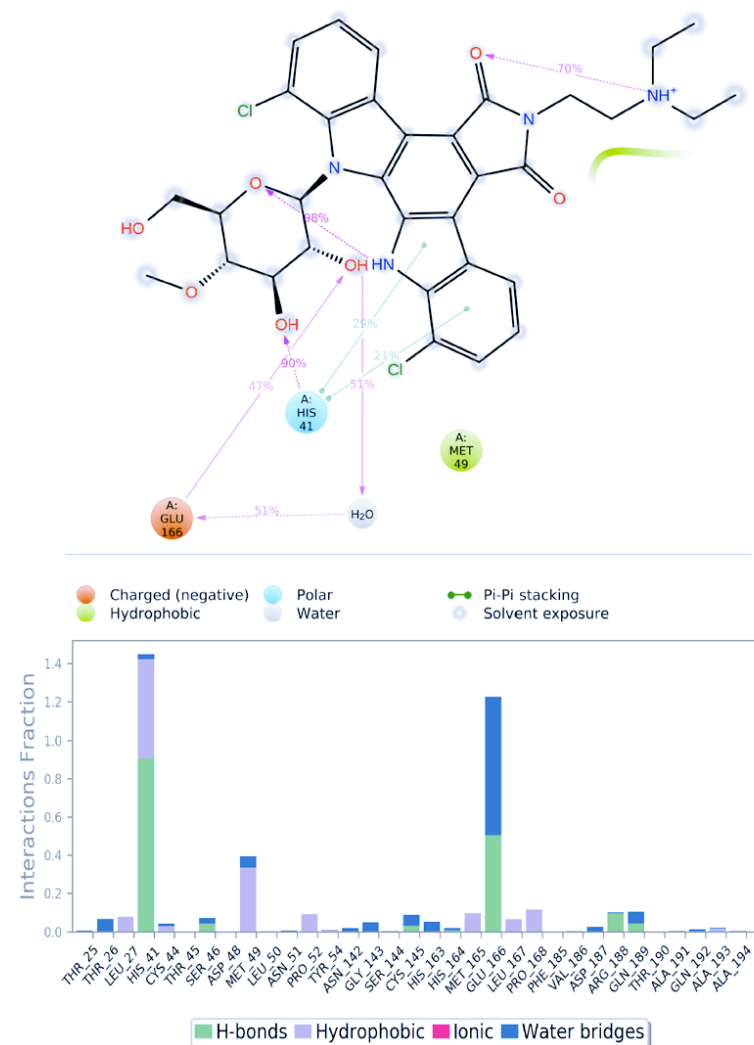
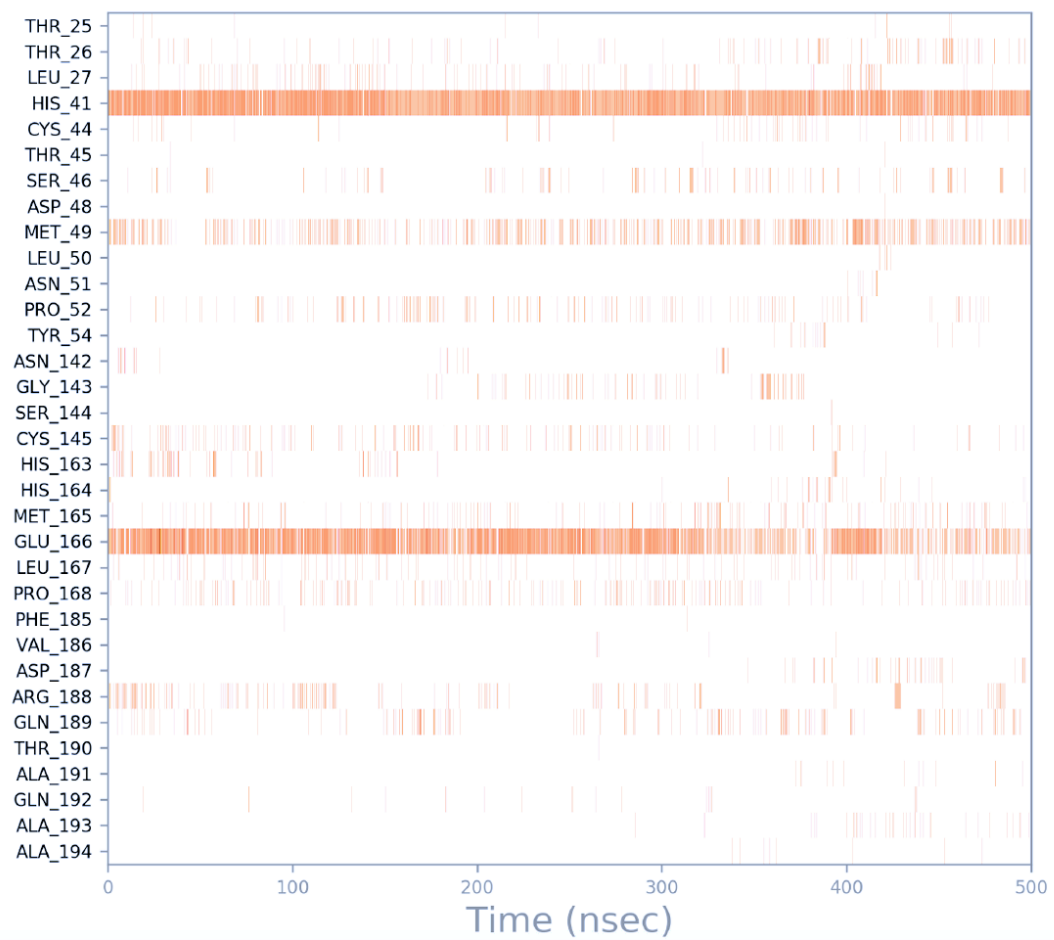


**Figure S3.** Ligand interactions diagram for **Bms181176-14**

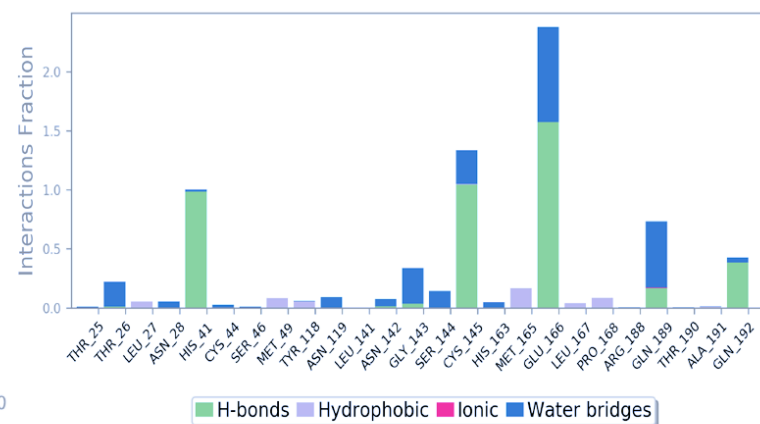
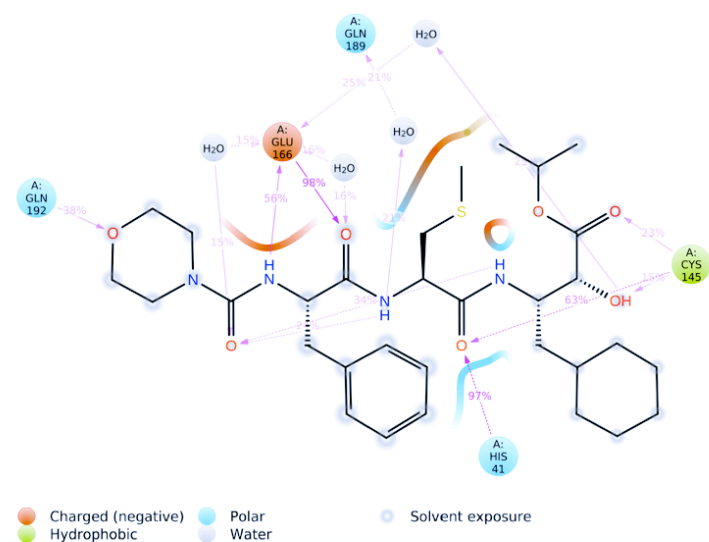
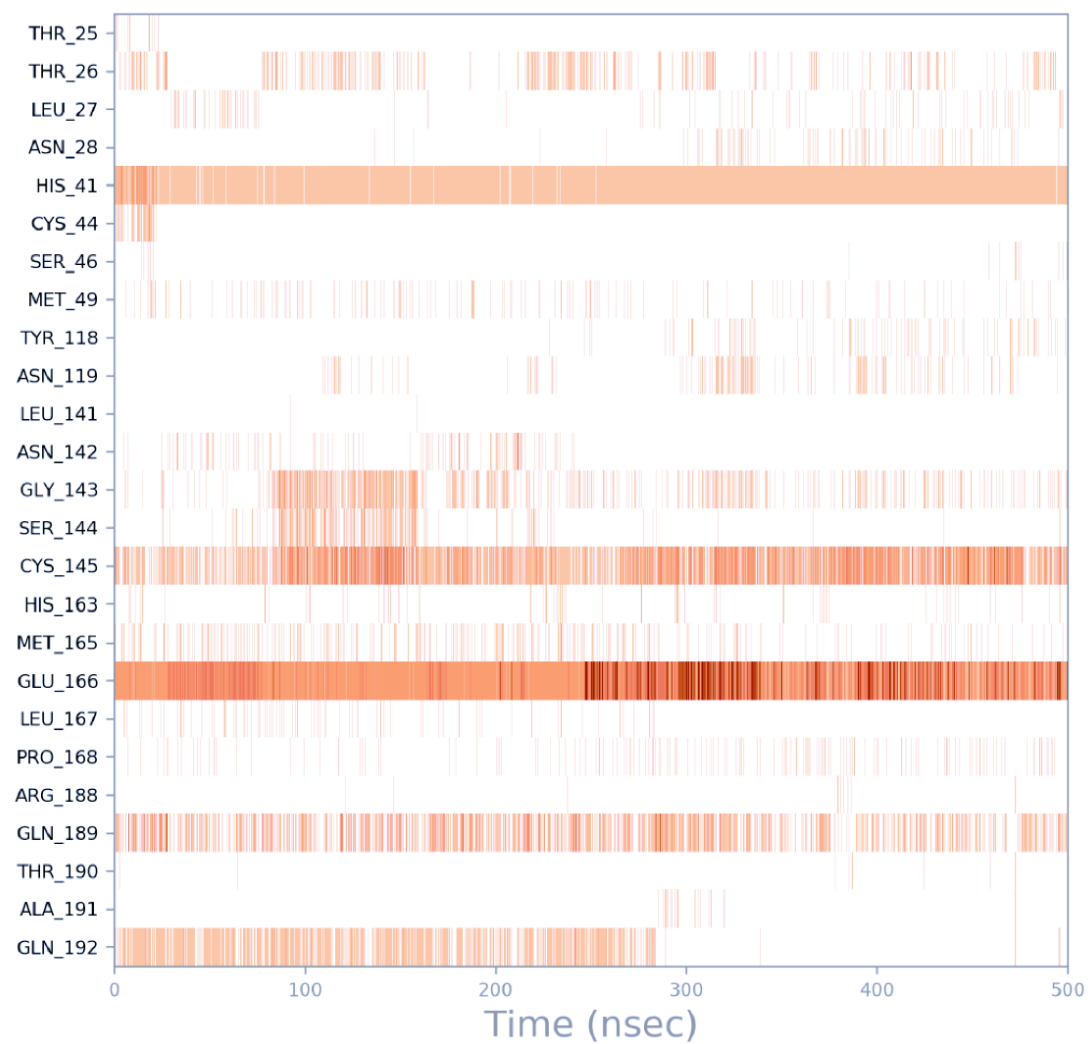


**Figure S4.** Ligand interactions diagram for **Terlakiren**

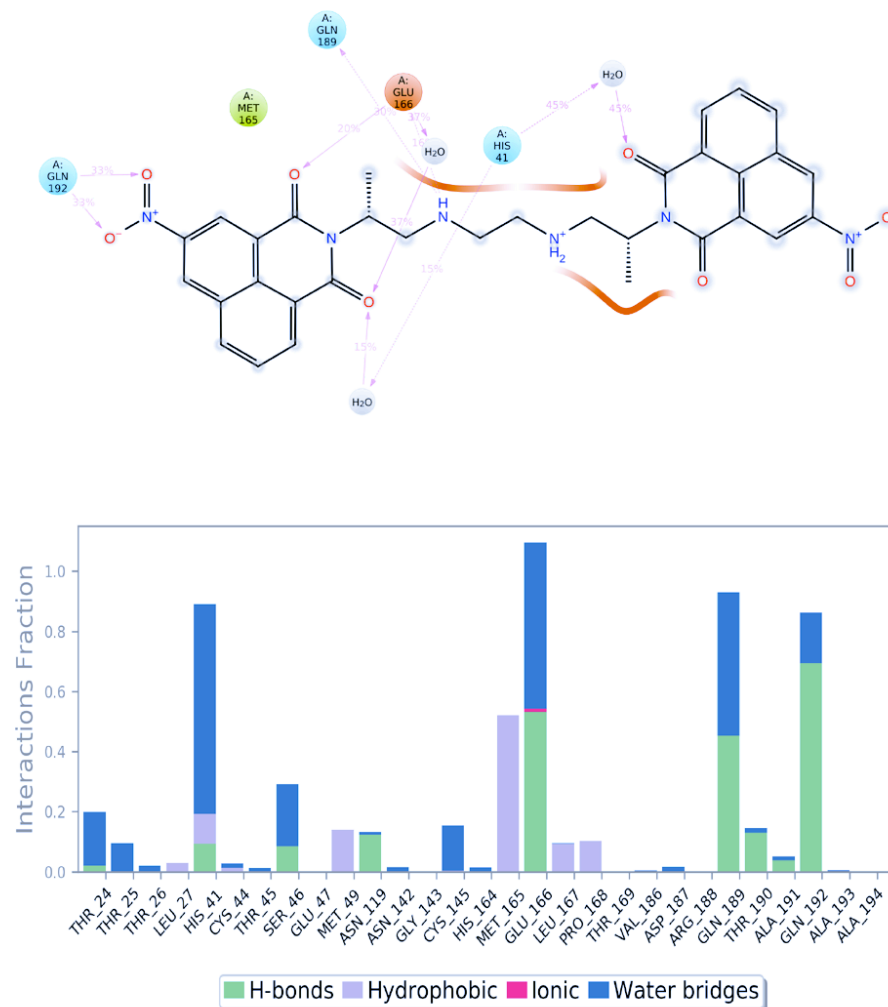
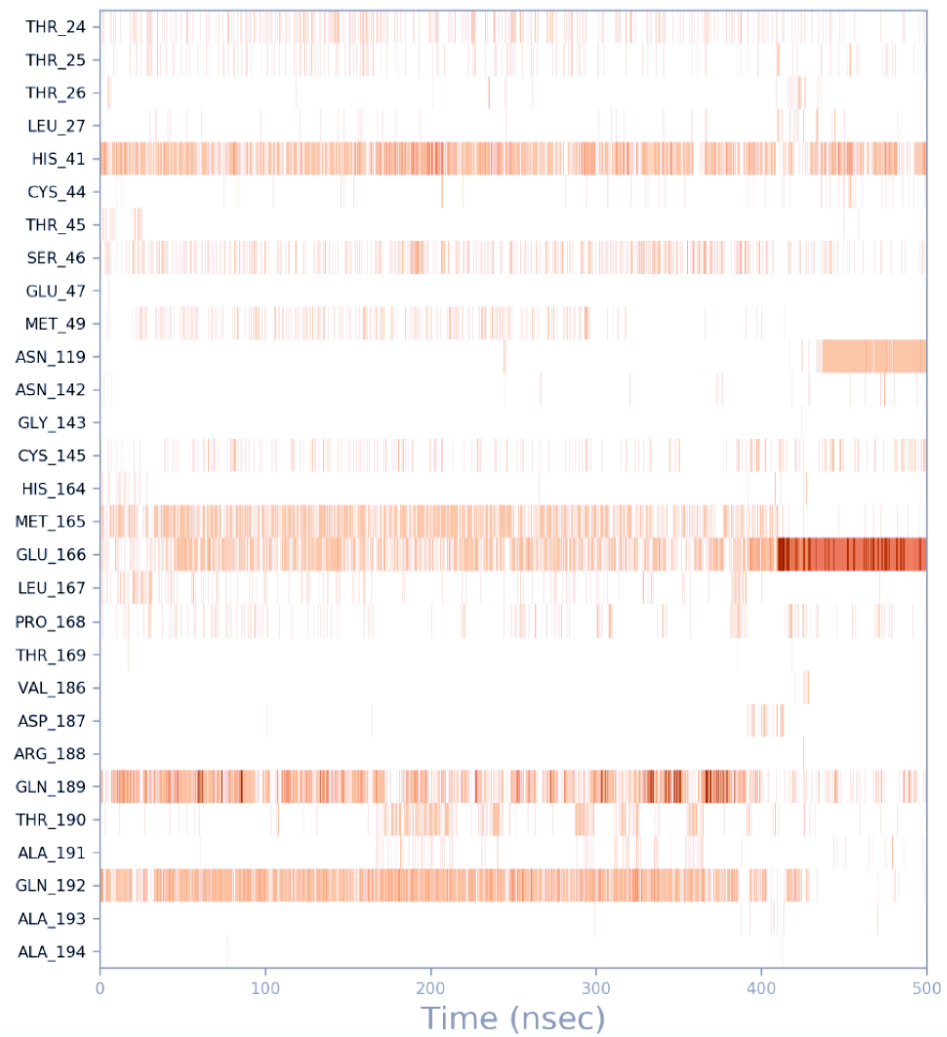


**Figure S5.** Ligand interactions diagram for **Bisnafide**



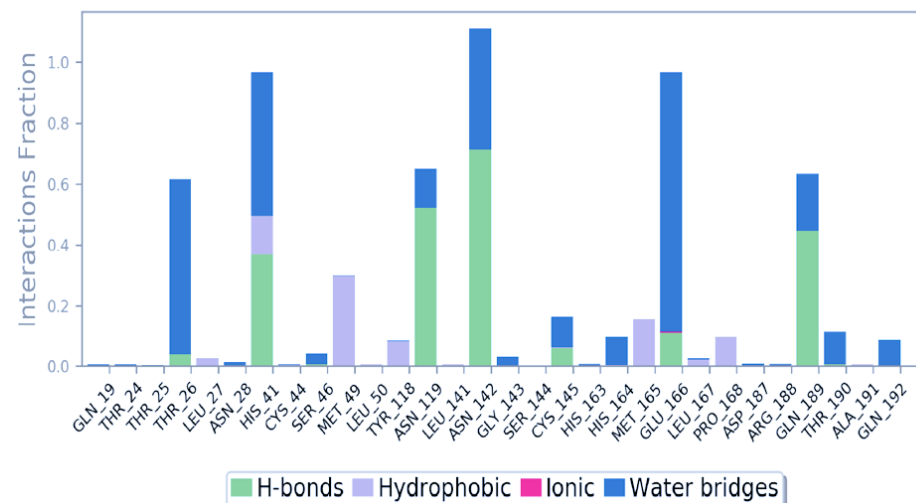
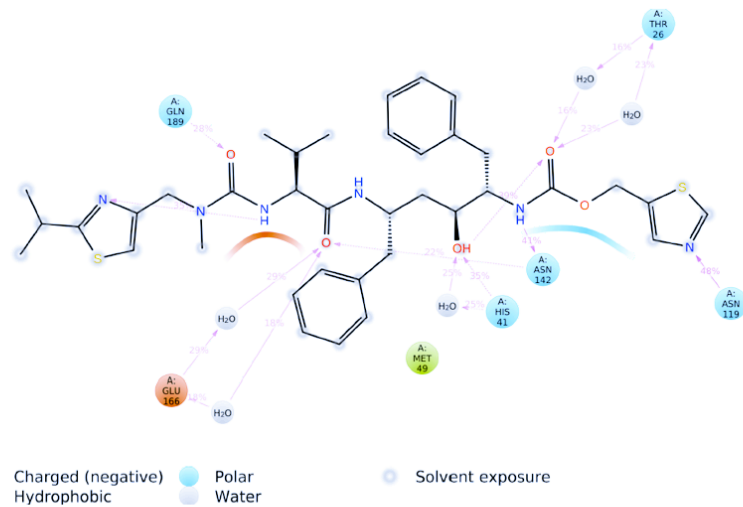
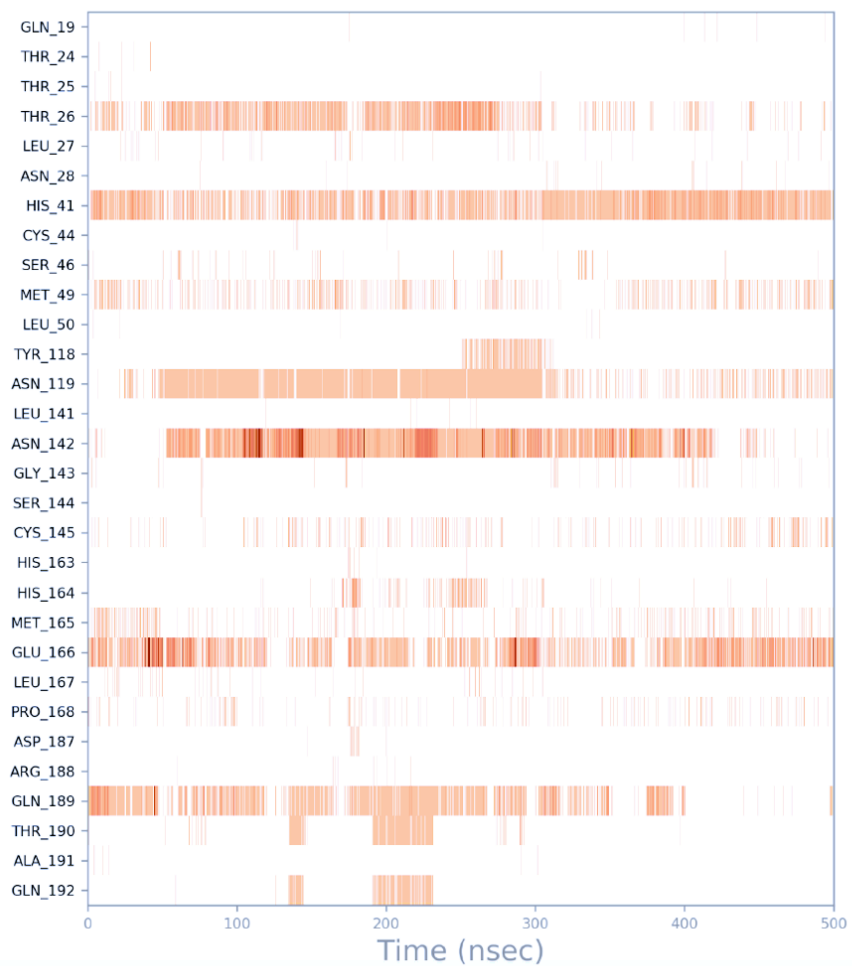
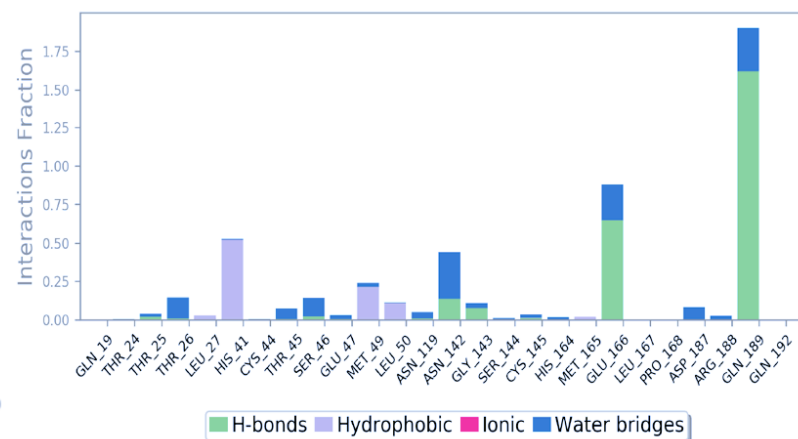
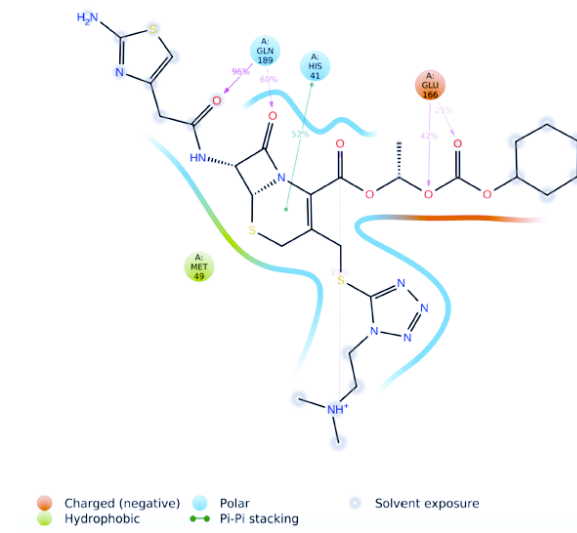
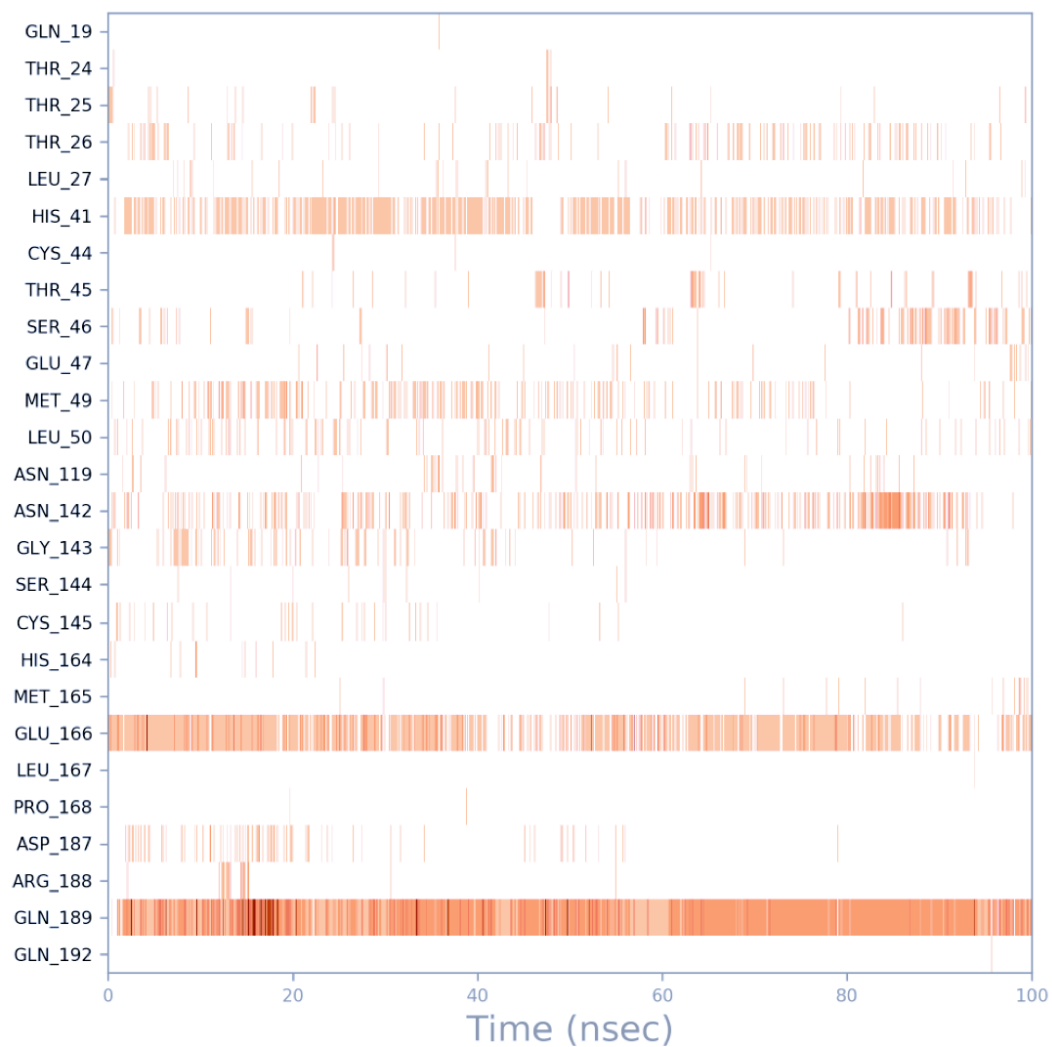
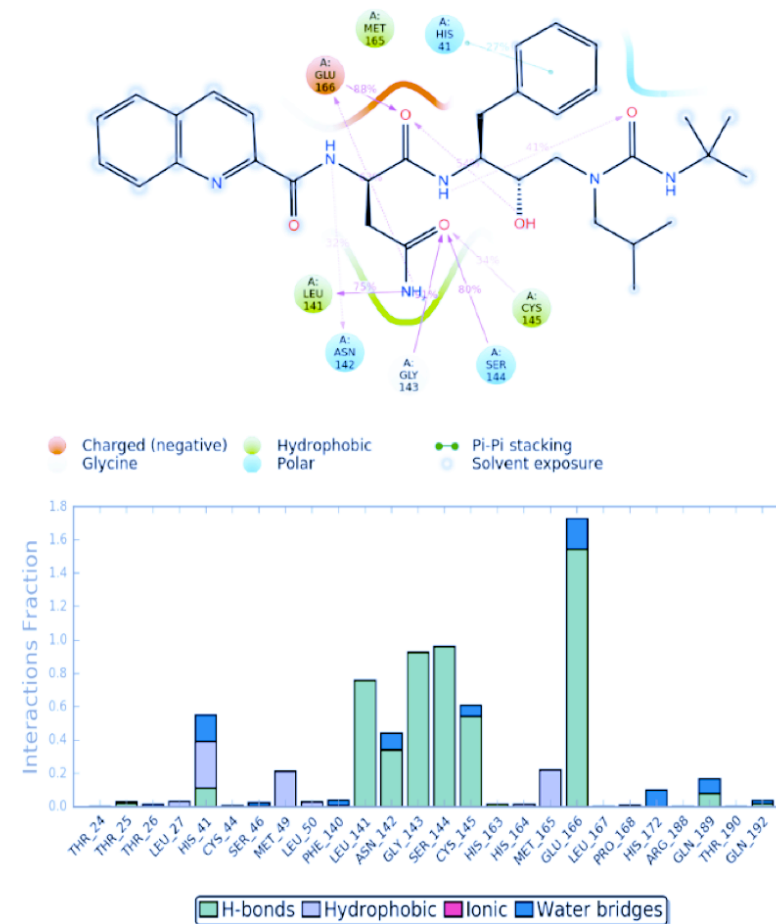
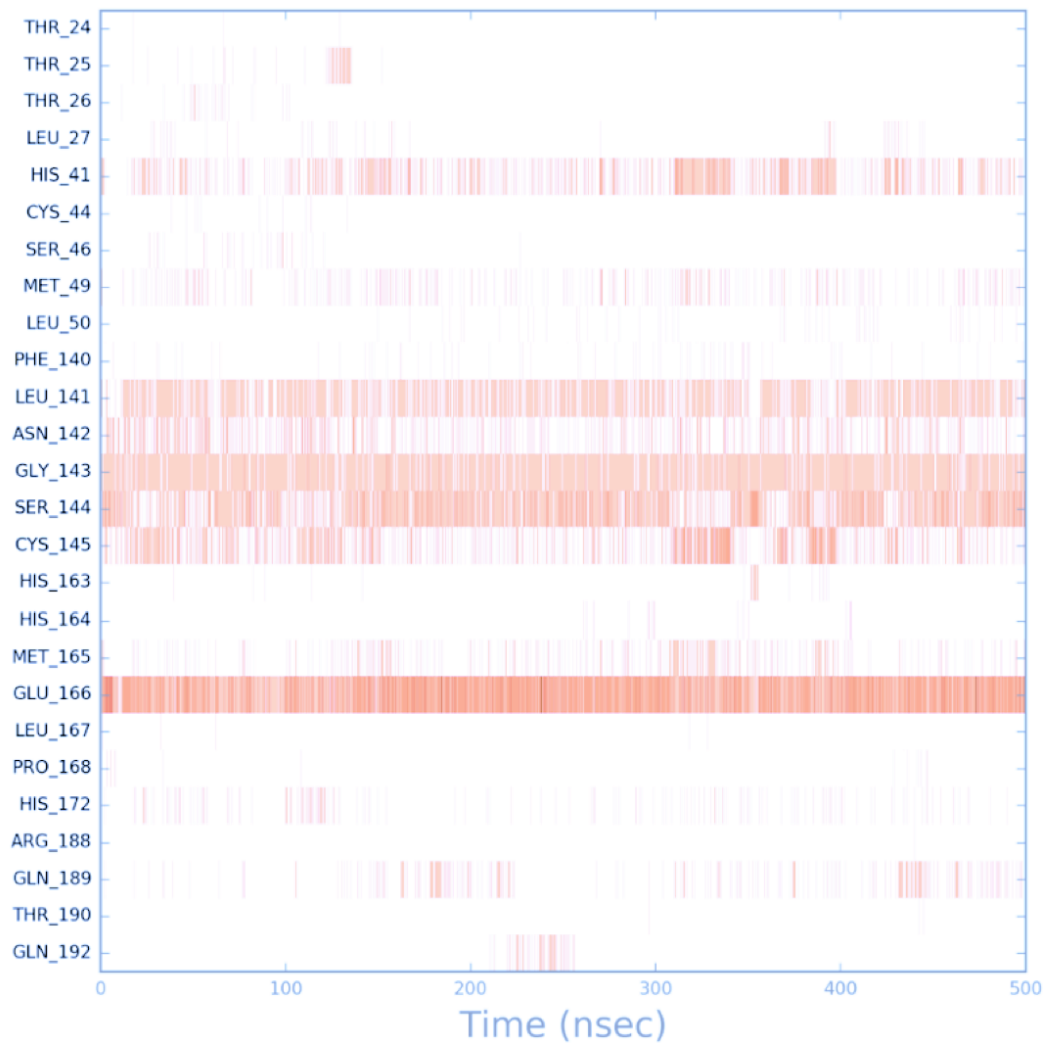


Figure S6. Ligand interactions diagram for Ritonavir



**Figure S7.** Ligand interactions diagram for **Cefotiam**



**Figure S8.** Ligand interactions diagram for **Telinavir**

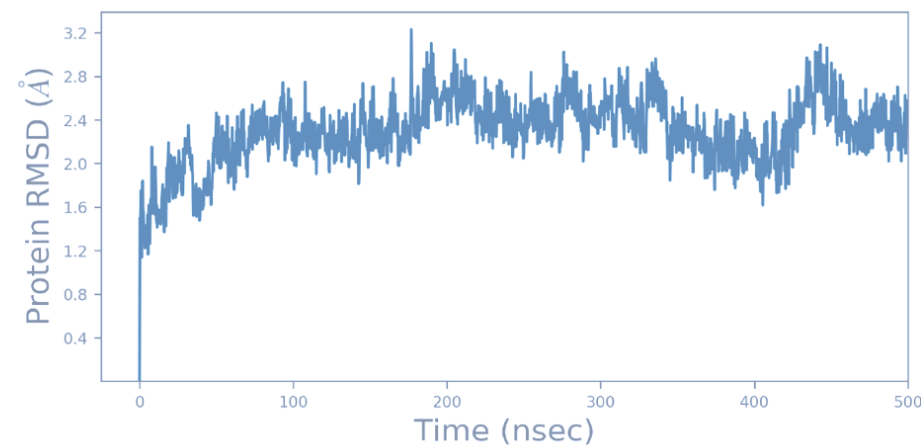
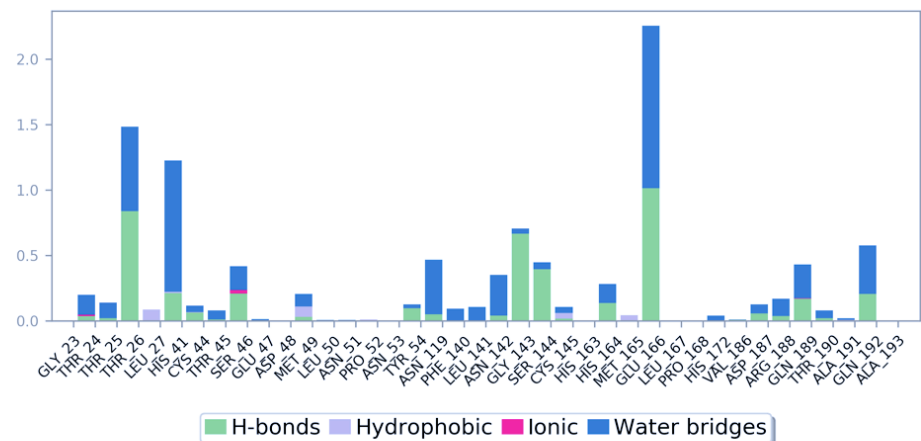


**Figure S9.** Ligand interactions diagram for **Rotigaptide**

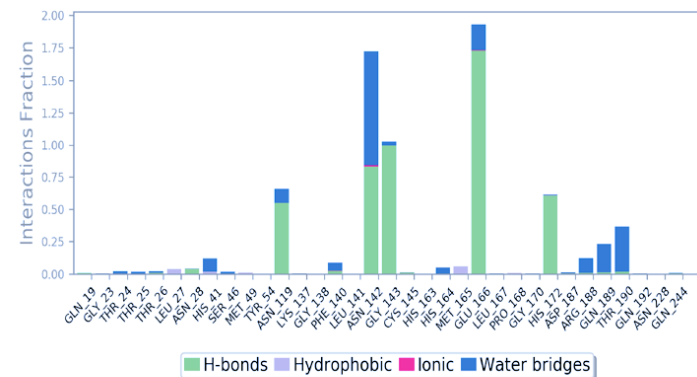
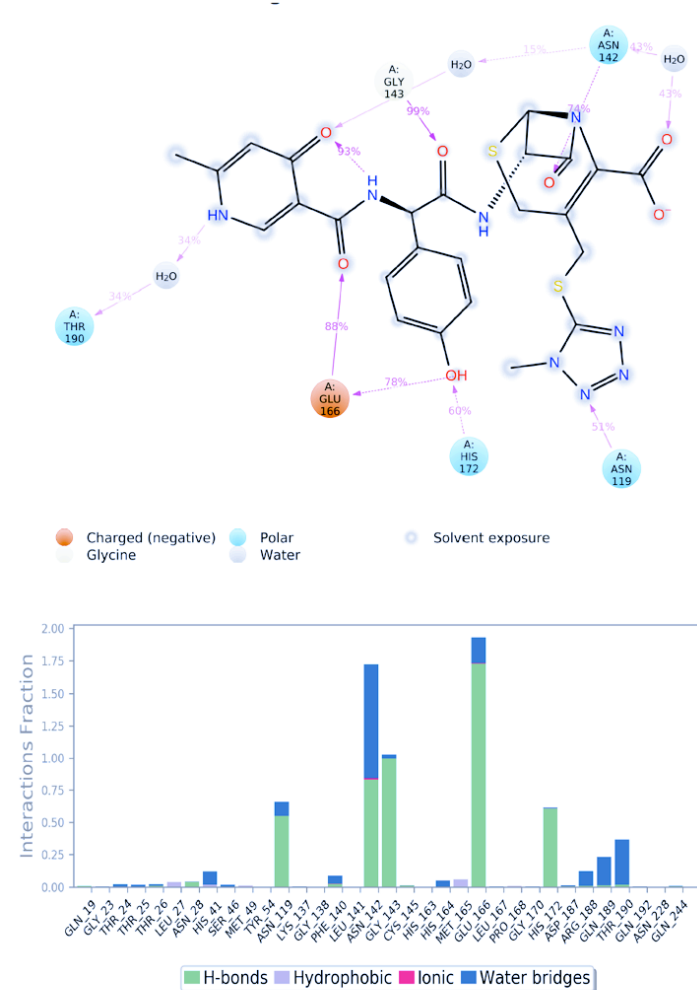
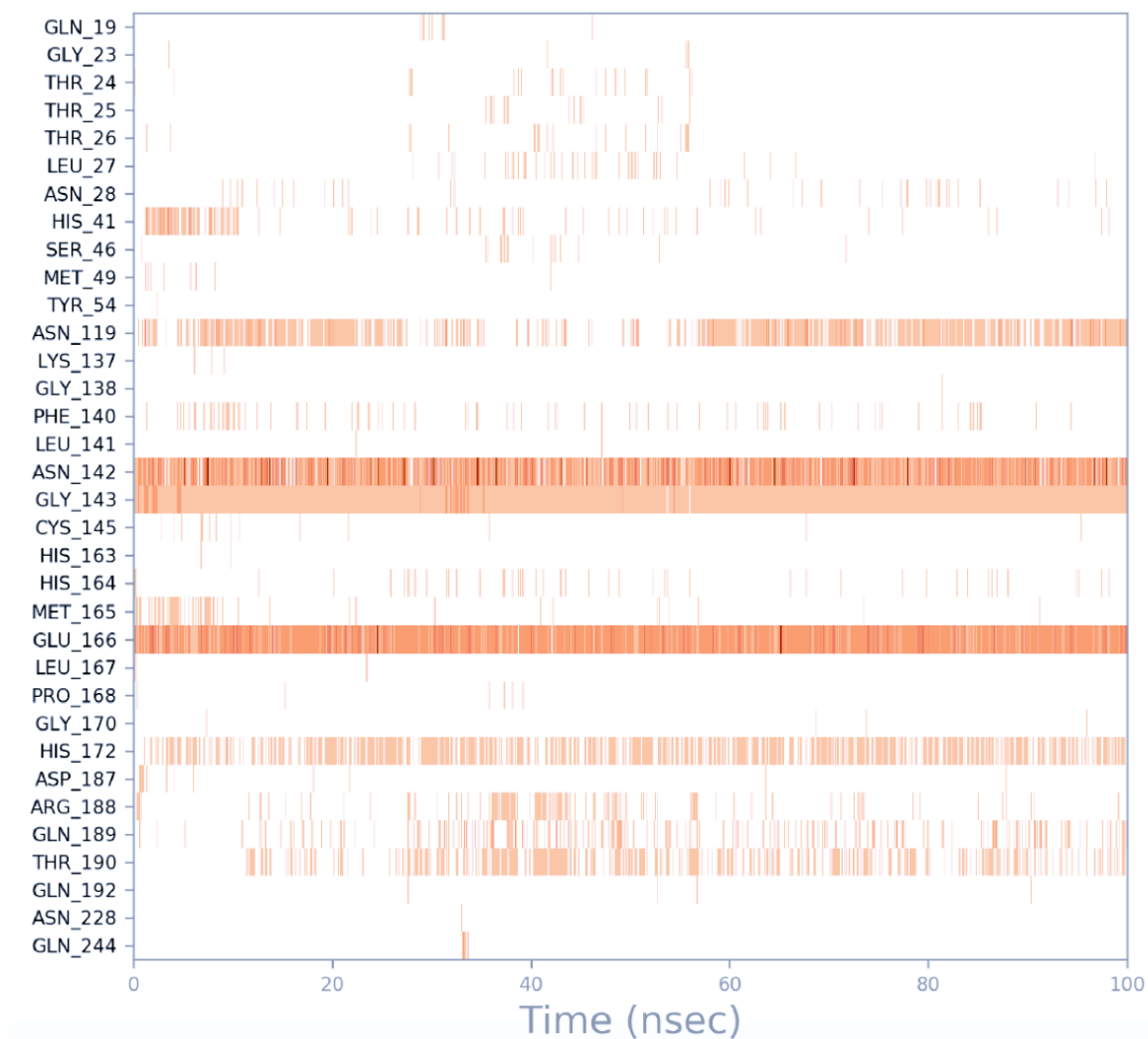


Figure S10. Ligand interactions diagram for Cefpiramide

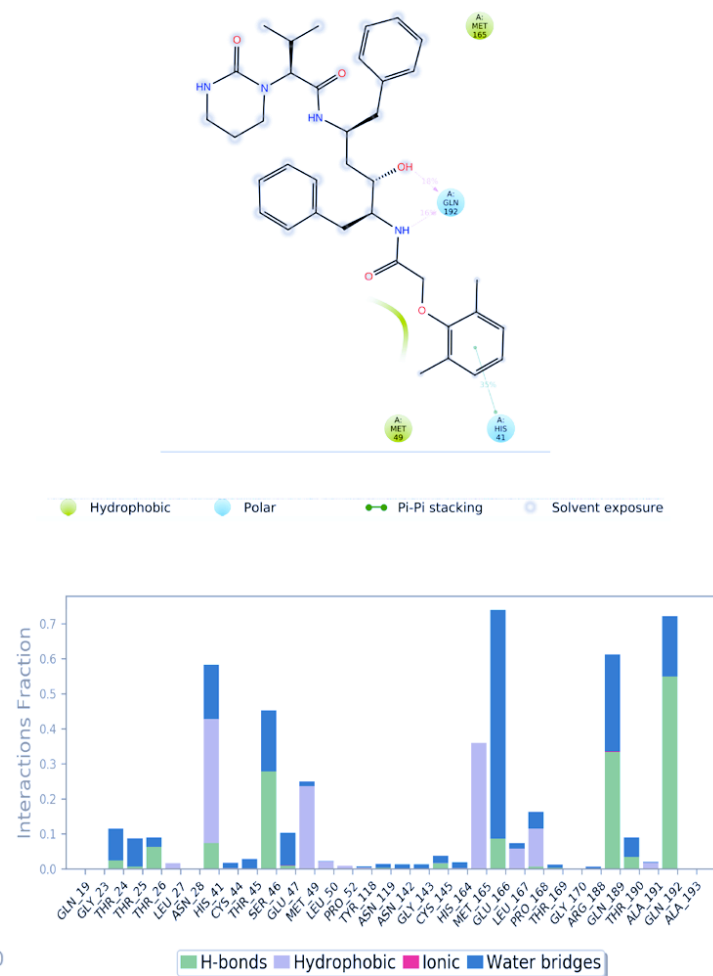
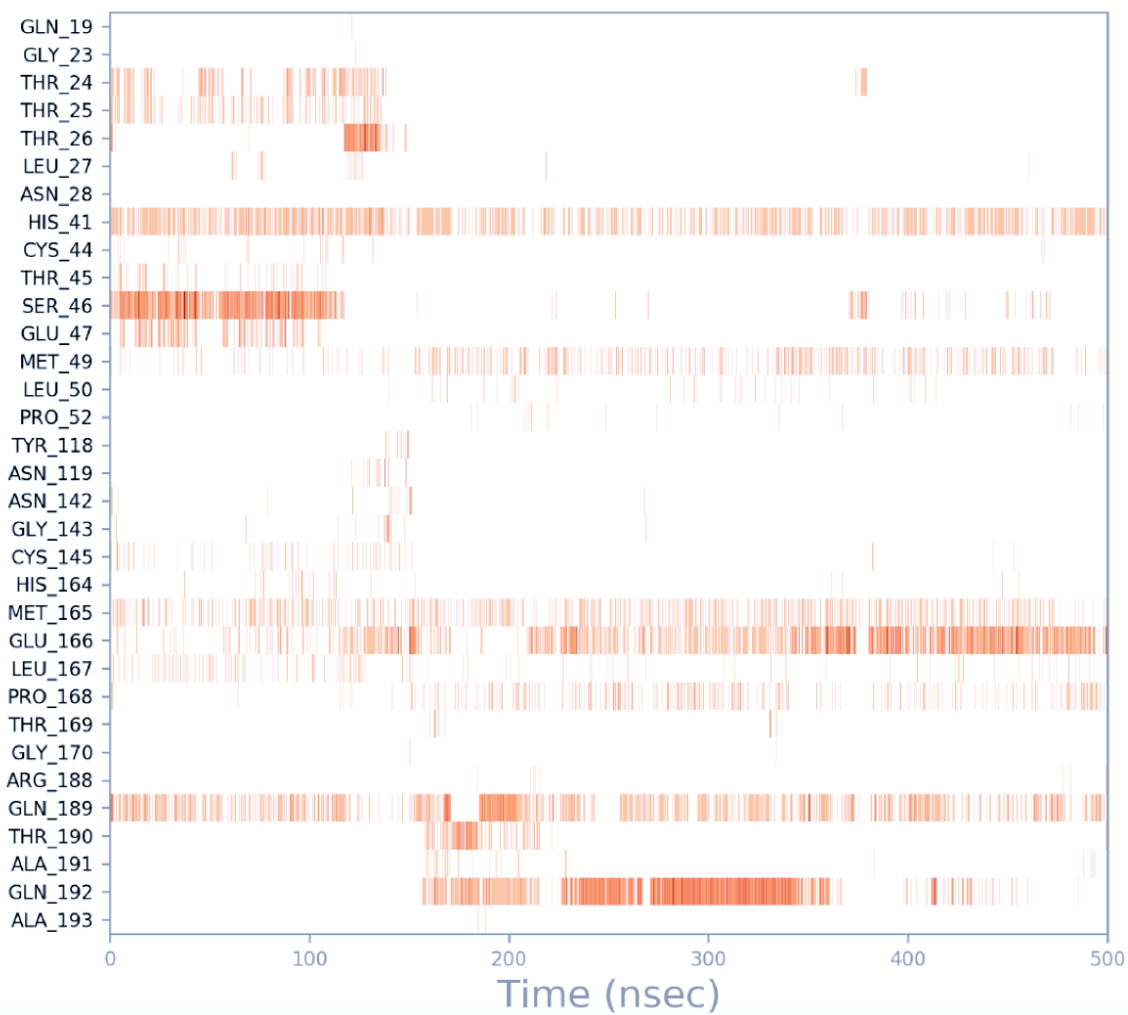
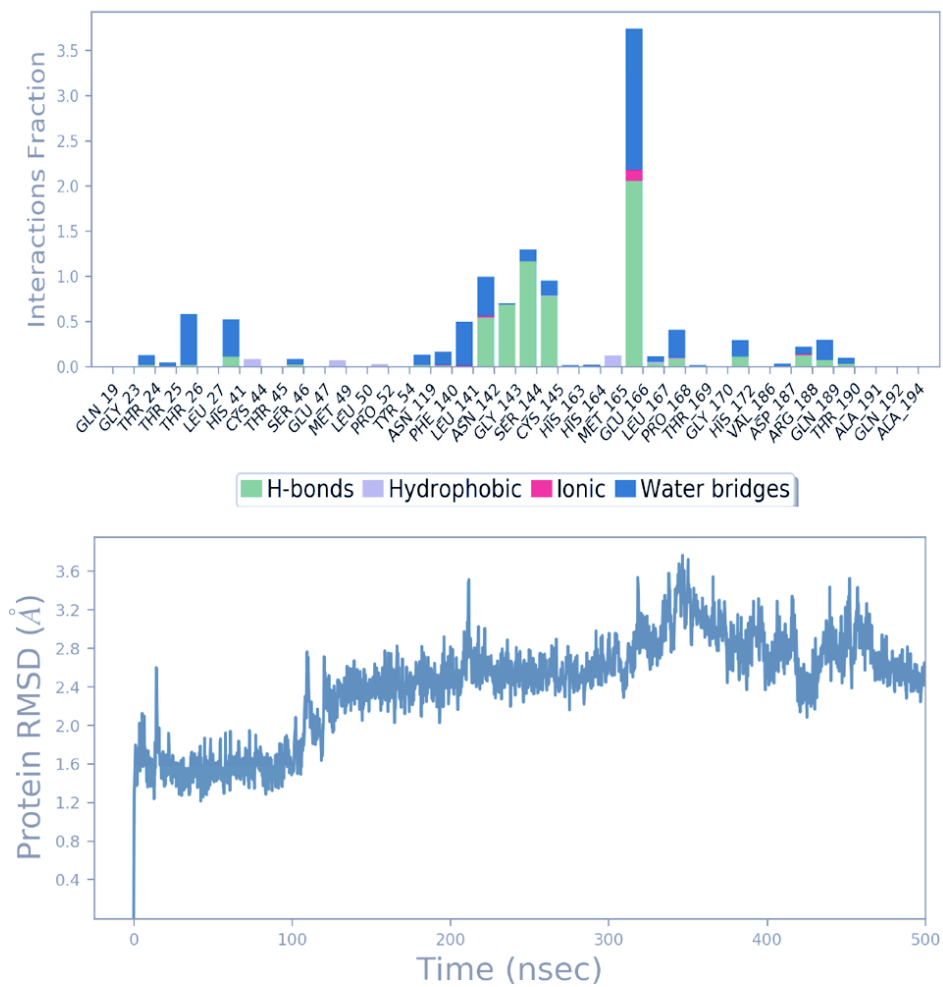


Figure S11. Ligand interactions diagram for Lopinavir



**Figure S12.** Ligand interactions diagram for **Pimelautide**

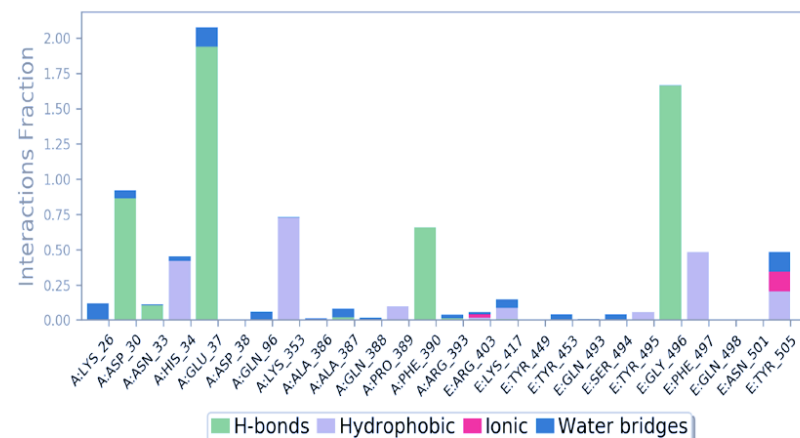
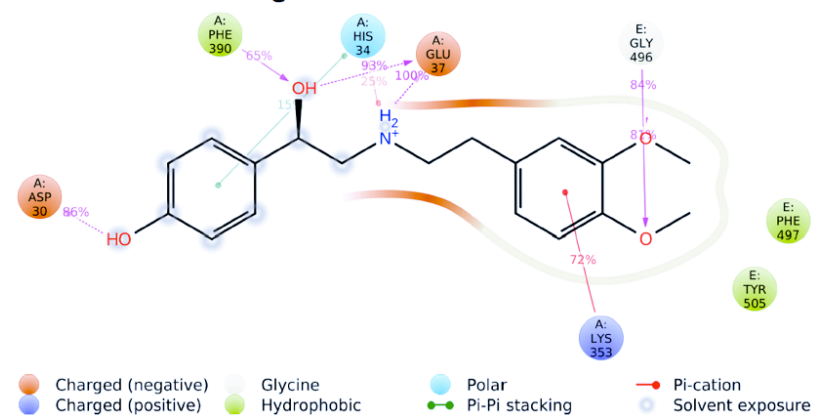
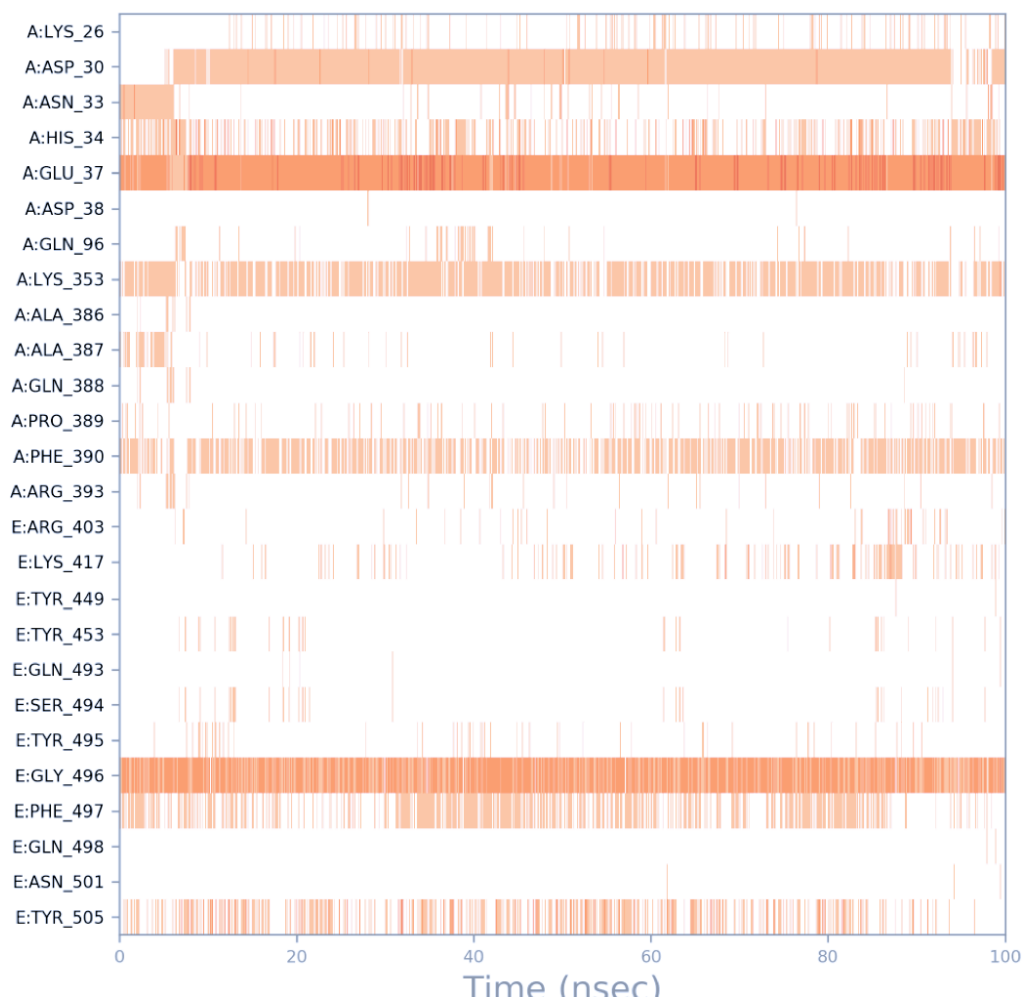


Figure S13. Ligand interactions diagram for Denopamine



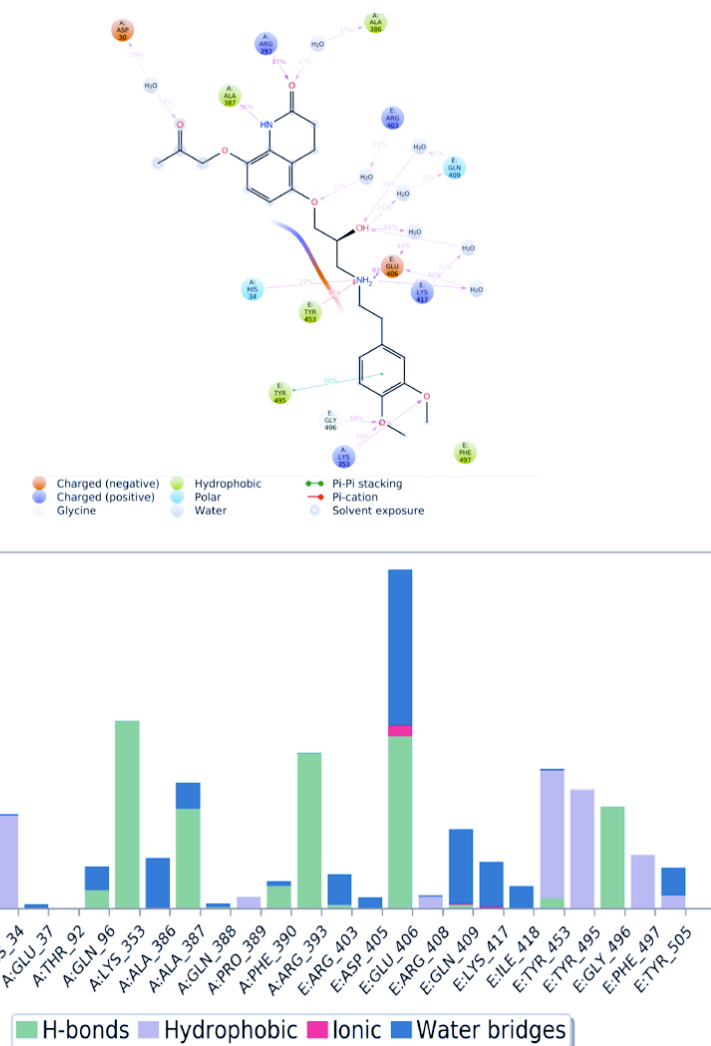
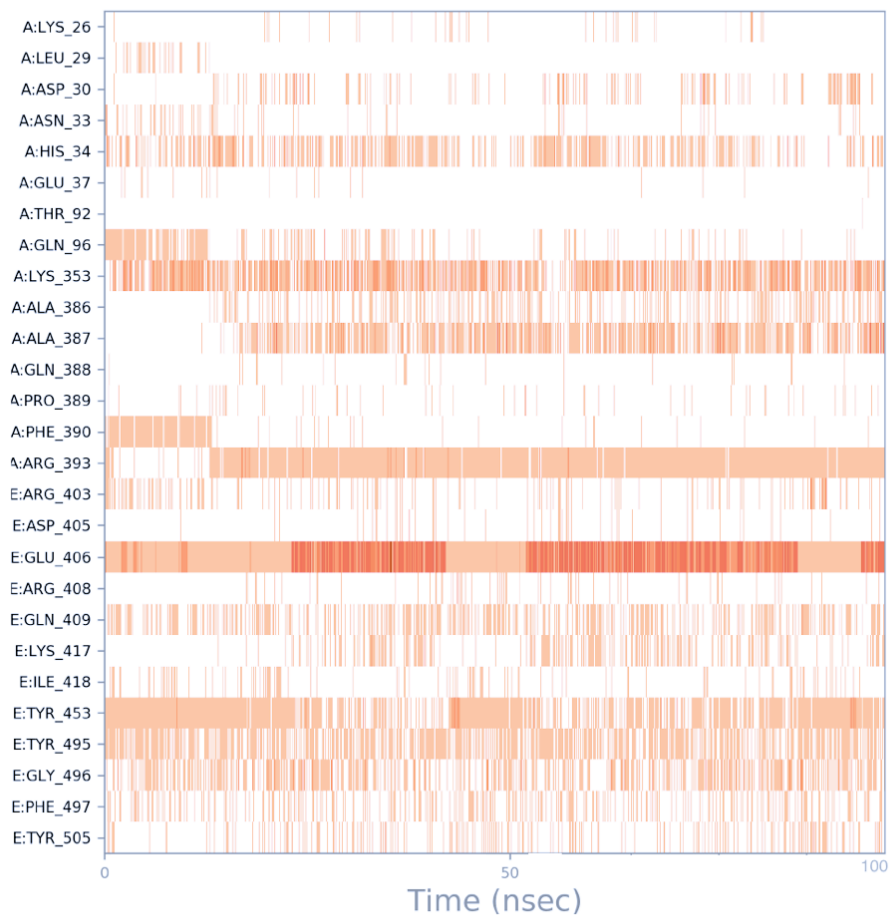


Figure S14. Ligand interactions diagram for **Bomotelol**

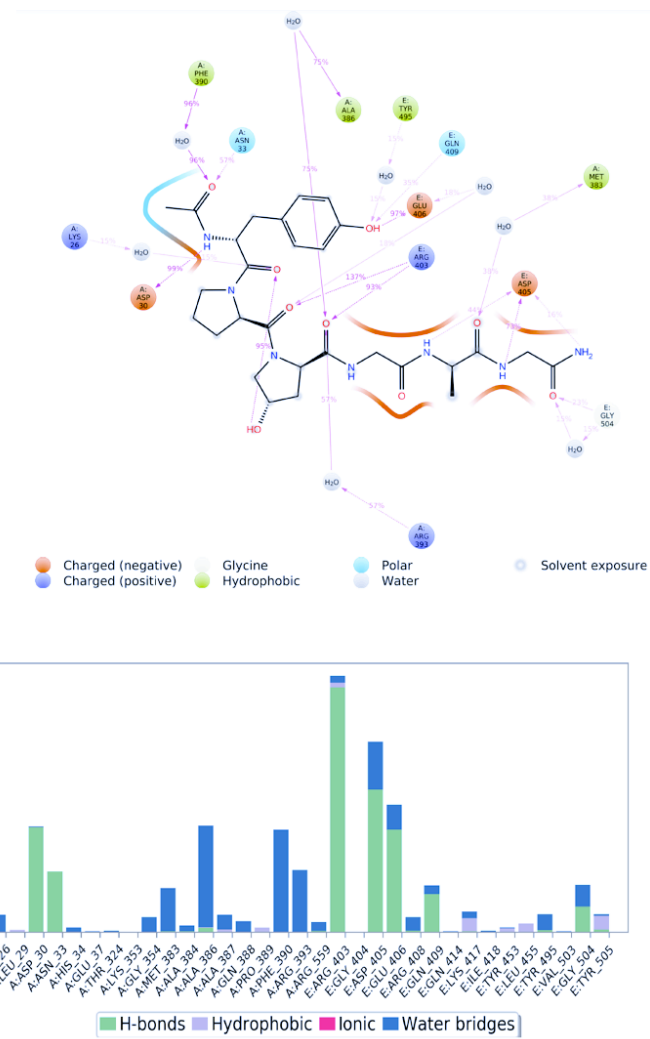
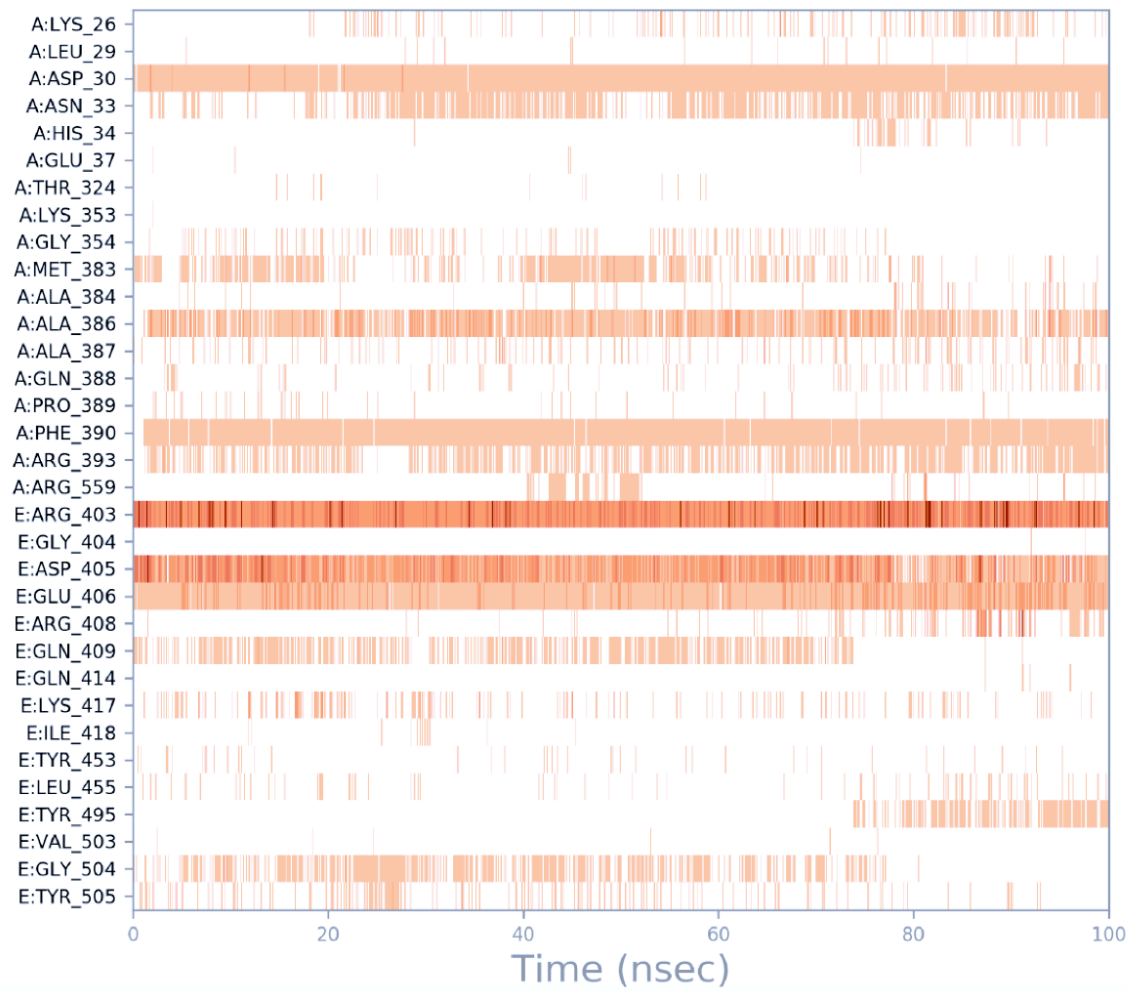


Figure S15. Ligand interactions diagram for Rotigatide

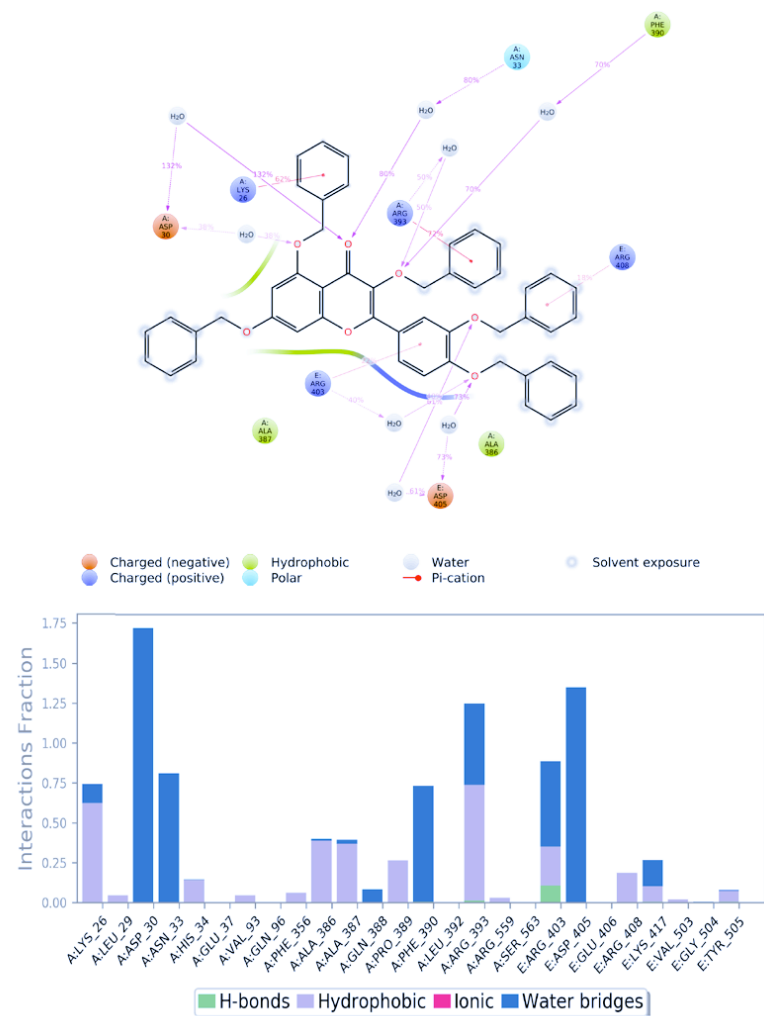
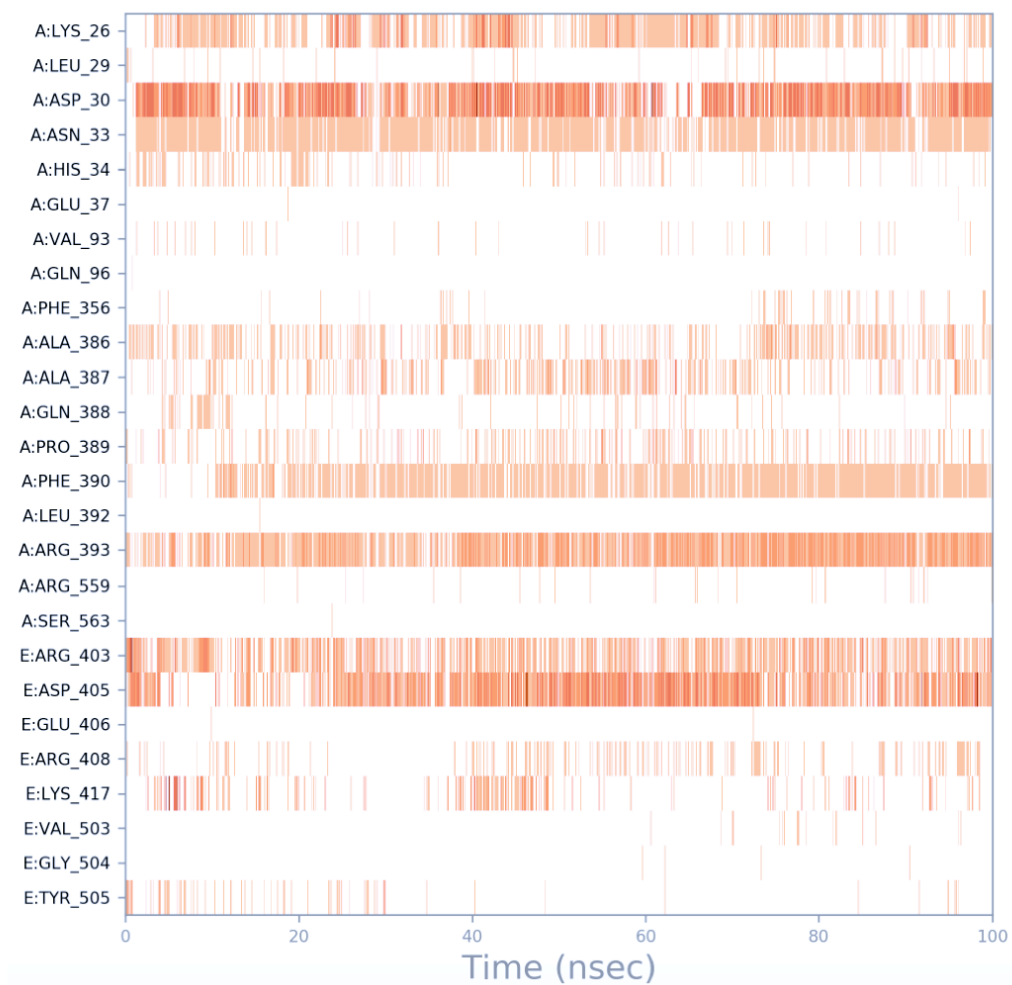


Figure S16. Ligand interactions diagram for Benzquercin